Plant disease recognition using fractional-order Zernike moments and SVM classifier

Thesis submitted in partial fulfillment of the requirements for the award of the degree of

Master of Engineering

in

Computer Science and Engineering

Submitted by

Parminder Kaur
(Roll no: 801532039)

Under the supervision of

Dr. Husanbir Singh Pannu

Lecturer, CSED

Computer Science and Engineering Department

Thapar University
Patiala-147004, Punjab, India

May 2017

Certificate

I hereby certify that the work, which is being presented in the thesis, entitled "*Plant disease recognition using fractional-order Zernike moments and SVM classifier*", in partial fulfillment of the requirements for the award of the degree of *Master of Engineering* in *Computer Science and Engineering* submitted in Computer Science and Engineering Department of Thapar University, Patiala, is an authentic record of my own work carried out under the supervision of *Dr. Husanbir Singh Pannu* and refers other researcher's work which are duly listed in the reference section.

The matter presented in this thesis has not been submitted for award of any other degree of this or any other University.

Parminder Kaur

Parminder Kaur

This is to certify that the above statement made by the candidate is correct and true to the best of my knowledge.

HS Pannu

Dr. Husanbir Singh Pannu
Lecturer, CSED

Abstract

Orthogonal moments have a vital role in the field of digital image processing and analysis. These moments are derived from statistically independent orthogonal polynomials and can be continuous or discrete. Major continuous orthogonal moments are Zernike, Pseudo-Zernike and Legendre moments and the primary discrete moments includes Krawtchouk, Tchebichef and Racah moments. In almost all researches till date, orthogonal moments are used with order having integer value, however, there is very less research on application of orthogonal moments with non-integer order which are also known as fractional-order orthogonal moments. Orthogonal moments with integer-order are a special case of fractional-order orthogonal moments. Each orthogonal moment can be made of fractional-order type by replacing integer order with real order. This study proposes the use of fractional-order Zernike moments in the recognition of grape leaf diseases and comparative analysis of these moments with integer-order Zernike moments is also presented. After extensive experiments, it can be said that the proposed technique is more robust to image noise and shows higher recognition rate (95.12% at order 30) compared to conventional techniques.

Keywords: fractional-order polynomials, orthogonal moments, fractional-order Zernike moments (FZM), Zernike moments (ZM), image recognition

Acknowledgement

First, I would like to express my deep gratitude to my supervisor **Dr. Husanbir Singh Pannu** for their invaluable advice and encouragement at every step of my ME program. Without their unfailing support and belief in me, this thesis would not have been possible. Their contribution to this thesis goes well beyond their role as an academic supervisor and includes constant support on a personal level without which this journey may never have been completed. And for this, I am truly grateful. They are great mentor for my life as well.

I would like to express my gratitude to **Dr. Maninder Singh**, Head of Computer Science and Engineering Department and **Dr. Ashutosh Mishra**, P.G. coordinator for their constant motivation and inspiration that encouraged me for the thesis work.

I would also like to give special acknowledgement to my fellow colleagues and staff members who were always there in the need of the hour and provided with all the help and facilities, which I required for the completion of thesis work.

Finally, I would like to express my sincere and deep gratitude to my parents, friends and family members for their love, encouragement, care and support. They showed me the right direction out of the blue, to help me stay calm in the oddest of times and keep moving even at times when there was no hope.

Parminder Kaur

Table of Contents

List of Figures

List of Tables

List of Notations

D^p_{nm}, D^c_{nm}	$(n+m)^{th}$ order moments
$P_{nm}(r, \vartheta)$	Jacobi fourier moments
$J_n(\alpha, \beta, r)$	deformed or radial Jacobi polynomials
$G_n(\alpha, \beta, r)$	Jacobi polynomials
$w(\alpha, \beta, r)$	Weight function in Jacobi polynomials
b_n	Normalization constant
P_{xy}	Pseudo-Jacobi fourier moments
$J_x(r)$	Pseudo-Jacobi fourier radial polynomials
Z_{pq}	Zernike moments
$V^*_{pq}(r, \theta)$	Zernike and pseudo-Zernike polynomials
$V_{pq}(r, \theta)$	Complex conjugate of Zernike and pseudo-Zernike polynomials
$R_{pq}(r)$	Radial Zernike and pseudo-Zernike polynomials
PZ_{pq}	Pseudo-Zernike moments
$\varphi_{nm}(x, y)$	Basis function of Legendre moments
$P_n(x)$	n_{th} order of Legendre polynomials
$f(x, y), f(r, \theta)$	Image function
$G^\alpha_n(x)$	Gegenbauer polynomials
α	Scaling factor in Gegenbauer polynomials
α_k	Pochhammer symbol
$B^\alpha_{n,k}$	Coefficient matrix
$w^\alpha(x)$	Weight function in Gegenbauer moments
$C_n(\alpha)$	Normalization constant in Gegenbauer moments
$A_{n,m}, \tilde{A}_{nm}$	Gegenbauer moments
A_{xy}	Chebyshev fourier moments
$C_x(r)$	Chebyshev fourier radial polynomials
O_{pq}	Orthogonal fourier mellin moments
$Q_p(r)$	Orthogonal fourier mellin radial polynomials
L_{mn}	Laguerre moments
$L^\alpha_n(x)$	Discrete Laguerre polynomials
${}_1F_1(.)$	Generalized hyper geometric function
H_m	Gaussian-Hermite moments
$\hat{H}_m(x)$	Normalized Hermite polynomials
$P_n(x; \alpha, \beta)$	continuous Hahn polynomials
$J_v(x)$	Bessel function
B_{nm}	Bessel fourier moments

H_{mn}	Radial harmonic fourier moments
$R_m(r)$	Radial kernal function of radial harmonic fourier moments
$x_i(G)$	parent vector of population G
F_{pq}	Fractional order Zernike Moments
A_{pq}	Fractional order Zernike polynomials
A_{pq}	Complex conjugate of fractional order Zernike polynomials
$B_{p,q}$	Radial fractional-order Zernike polynomials
$I(x,y), I(r,\theta)$	Image function in fractional-order moments
δ_{ab}	Kronecker delta
α	Real number used for making integer order fractional
n, p	Moment order
m, q	Repetition
r	Length of vector from origin to (x, y)
D	Diameter of circle on which image is mapped
N	Dimension of image
x_i, y_i	Mapped pixel coordinates

List of Abbreviations

BFM	Bessel Fourier Moments
CFM	Chebyshev Fourier Moments
CHM	Continuous Hahn Moments
FZM	Fractional-order Zernike Moments
GHM	Gaussian Hermite Moments
GM	Gegenbauer Moments
JFM	Jacobi Fourier Moments
LaM	Laguerre Moments
LM	Legendre Moments
OFMM	Orthogonal Fourier Mellin Moments
OM	Orthogonal Moments
PJFM	Pseudo-Jacobi Fourier Moments
PZM	Pseudo-Zernike Moments
RHFM	Radial Harmonic Fourier Moments
RR	Recognition Rate
SVM	Support Vector Machine
ZM	Zernike Moments

Chapter 1

Introduction

The work presented in this thesis mainly focuses on the recognition of various diseases present on the surface of grape plant leaves. So, for the recognition of diseases, a new approach of feature extraction using fractional-order Zernike moments is proposed. This chapter introduces with the various existing continuous orthogonal moments and the conventional ways of plant disease recognition.

Indian economy highly depends upon agricultural productivity. So, it is important to detect diseases present in plants as soon as possible and provide medicine accordingly. These diseases in plants are caused by malignant viruses, bacteria and fungus. If proper medicine is not provided on time then it can seriously affect the plants and consequently the product quantity, quality and productivity is also affected. It becomes nearly impossible to detect and analyze plants manually on a large scale of vegetation with full attention by an expert. Thus automation of disease diagnosis is required to make the procedure efficient through image processing. About 80-95% of the plant diseases reflect on the leaves, so without loss of generality, the leaf diagnose is sufficient for disease investigation. Figure (1-5) show some of the prominent leaf diseases. In this thesis, diseases related to grape leaves are identified using fractional-order Zernike moments (FZM). FZM is the improved version of ZM [1] which comes under continuous orthogonal moments. Other prominent continuous orthogonal moments include Legendre moments [1], Pseudo-Zernike moments [2], orthogonal fourier mellin moments [3] and gaussian Hermite moments [4, 5].

Figure 1.1: Alternaria disease

Figure 1.2: Cercospora disease

Figure 1.3: Red leaf disease

Figure 1.4: Yellow leaf disease disease

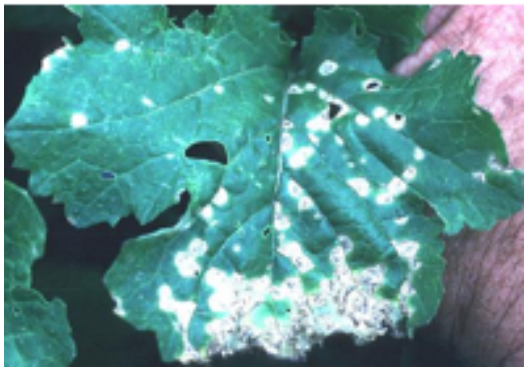

Figure 1.5: White leaf disease

Moments are the projections of image functions onto particular kernel functions. They can be defined in polar (equation (1.1)) as well as Cartesian coordinate system (equation (1.2)).

$$D^p_{nm} = \int_0^1 \int_0^{2\pi} G_{nm}(r,\theta) f(r,\theta) r dr d\theta \tag{1.1}$$

$$D^c_{nm} = \int \int_{R^2} G_{nm}(x,y) f(x,y) dx dy \tag{1.2}$$

where D^p_{nm} and D^c_{nm} represents the (n+m)th order moments of image functions $f(r,\theta)$ and $f(x,y)$ respectively. $n, m = 0, 1, 2, 3, ...$ and $G_{nm}(r,\theta)$ and $G_{nm}(x,y)$ denotes the basis function or kernel function. With change in kernel functions, different types of moments can be obtained. Now, these moments are said to be orthogonal if they satisfy the following equations (1.3 and 1.4):

$$\int_0^1 \int_0^{2\pi} G_{nm}(r,\theta) G_{st}(r,\theta) r dr d\theta = k_1 \delta_{ns} \delta_{mt} \tag{1.3}$$

$$\int_0^1 \int_0^1 G_{nm}(x,y) G_{st}(x,y) dx dy = k_2 \delta_{ns} \delta_{mt} \tag{1.4}$$

here k_1 and k_2 are normalization coefficients and δ_{ns} represents Kronecker delta, otherwise the moments will become non-orthogonal. Non-orthogonal moments include complex moments (with kernel function $G_{nm}(x, y) = (x + iy)^n(x - iy)^m$), geometric moments ($G_{nm}(x, y) = x^n y^m$) and rotational moments ($G_{nm}(r, \theta) = r^n e^{-im\theta}$) which are defined in [6, 7]. Non-orthogonal moments face difficulties in image reconstruction due to lack of orthogonal nature. They are highly sensitive to noise and information redundant also. However, orthogonal moments are rotation, scaling and translation invariant, robust to image noise and show very less information redundancy. Due to these advantages, they have been used in various digital image processing areas such as face recognition [8], image watermarking [9], palm print and iris identification [10, 11], image reconstruction [12] and character recognition [13].

We have picked ZM for conversion to FZM because they are the most popular moments among other continuous orthogonal moments. They are also easy to implement and shows effective results in case of image representation capability. Moreover, they require lower computational precision to represent images. Before a detailed study of FZM, a short review of existing ZM and other continuous orthogonal moments are discussed in the following subsections. All existing orthogonal moments have integer orders since their corresponding polynomials' order are of integer type. However, recently in [14], authors have introduced the concept of fractional orthogonal moments and discussed their properties while applying them on image reconstruction and face recognition. They have taken the example of shifted Legendre moments and converted them into fractional form in both Cartesian and polar coordinate space. The results obtained using fractional orthogonal moments are much better than normal existing orthogonal moments. So, motivated from that work, this work proposes fractional order Zernike moments and their application in recognition of diseases present on grape leaf. Moreover, to the best of our knowledge, fractional-order Zernike moments are introduced here for the first time and also orthogonal moments have not been used for plant disease detection before.

Table 1.2: Application areas of image moments

Moments	**Application Areas**	**References**	**Enhancement**
Jacobi Fourier Moments	image watermarking, image reconstruction, mammogram classification (discrete implementation of Jacobi Moments)	[27], [15], [28]	[29, 30]

Pseudo-Jacobi Fourier Moments	image reconstruction, image recognition and reconstruction	[16], [21]	-
Zernike Moments	Texture Analysis, gurumukhi character recognition, Chinese character recognition, fingerprint recognition, palm print verification, iris identification, face recognition, image reconstruction, traffic sign recognition, Offline handwritten signature verification, near-duplicate video retrieval, pigs posture recognition, facial expression recognition, Ground traffic signs recognition, Indian sign language gesture recognition	([31], [32]), [33], [34], [17], [10], [11], ([35], [36], [37]), [38], [39], [40], [41], [42], [43], [44], [45]	[46, 47, 48, 49]
Pseudo-Zernike moments	face recognition, palm print verification, fingerprint recognition, image watermarking, Farsi handwritten character recognition, automatic target recognition, object contour detection	([50], [18]), [51], ([52], [53]), [54], [55], [56], [57]	[58, 59, 8, 60, 61, 62]
Gegenbauer Moments	Chinese character recognition	[20]	[63]
Chebyshev Fourier Moments	image recognition, image reconstruction	[21], [64]	[65]
Orthogonal Fourier Mellin Moments	Pattern Recognition, character recognition of alphanumeric characters	[3], [13]	[66, 67, 68, 69]
Laguerre Momente	Image Reconstruction	[22]	-

Legendre Moments	face recognition, palm print authentication, iris verification, classification of 2D polyacrylamide gel electrophoresis, texture analysis, 3D object images classification, histogram representation, vehicle recognition, image watermarking, line fitting in noisy image, incorporation of geometric shape priors in region based active contours, image indexing and retrieval from image DB, finger crease pattern recognition, noise removal from ECG signals, reconstruction of noisy medical images	[19], [70], [71], [72], [73], [74], [75], [76], [77], [78], [79], [80], [81], [82], [83]	[84, 85, 86, 67, 87, 88, 89, 90]
Gaussian-Hermite Moments	moving objects' recognition, iris image recognition, image watermarking, image reconstruction, singular point detection in fingerprint classification, 3D face recognition, face recognition, license plate character recognition, human motion detection, character recognition, image compression	[23], ([91], [92]), [9], [93], ([94], [95], [96]), [97], [98], [99], [100], [23], [101] (discrete implementation)	[102]
Continuous Hahn Moments	mapping of polynomials	[24]	-
Bessel Fourier Moments	image reconstruction and recognition	[25]	-

Radial Harmonic Fourier Moments	image reconstruction, content based retrieval, image recognition, image watermarking, Chinese chess character recognition	[103], [104], [105], [106], [107]	[108, 106]

1.1 Continuous Orthgonal Moments

Orthogonal means statistically independent or have mutually perpendicular basis set. Orthogonal Moments make use of orthogonal polynomials as their kernel functions in the moment integral. The scalar quantities which are used to depict a function and capture its important features are known as moments. In 1962, M.K. Hu was the first person who introduced the use of moment invariants in image analysis and object recognition in his paper [109]. Initially, geometric moments and regular moments were used for the image analyses which are non-orthogonal in nature. Due to non-orthogonality, these moments are highly information redundant and do not provide good results in case of image recovery. To overcome the problems of geometric moments, Teague [1] gave the idea of using orthogonal moments for image analysis which give much better results than non-orthogonal moments. Orthogonal moments show very less information redundancy and are invariant to rotation, scaling and translation as well as robust to image noise. These advantages of orthogonal moments leads to many applications like fingerprint recognition [17], image reconstruction [12], character recognition [33], image watermarking [110] etc. Orthogonal Moments can be broadly classified as Continuous and Discrete Orthogonal Moments. Moments' classification described by [6] is shown in figure (1.6). Table (1.1) shows the continuous orthogonal moments, their abbreviations and references. More references are presented in the form of graph shown in figure (1.8). Figure (1.7) shows all continuous orthogonal moments discussed here and their applications areas, references and enhancement references are shown in table (1.2). The following subsections describe about various continuous orthogonal moments.

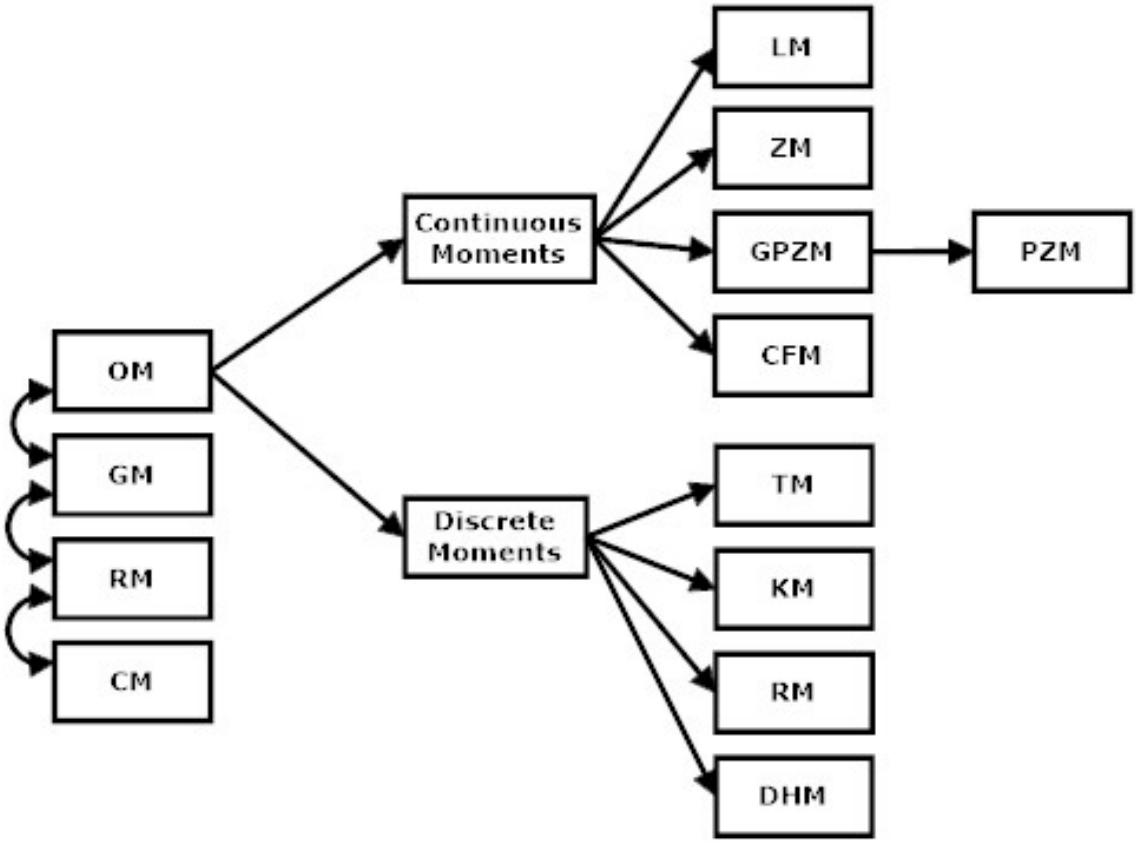

Figure 1.6: Broad classification of continuous and discrete orthogonal moments

1.1.1 Jacobi Fourier Moments

The kernel of Jacobi Fourier Moments ($P_{nm}(r, \vartheta)$) comprises of two independent function sets: (1) Deformed Jacobi polynomial($J_n(\alpha, \beta, r)$) to be radial function and (2) Fourier exponential factor ($exp(jm\vartheta)$) to be angular function. So, JFM are defined as in equation (1.5):

$$P_{nm}(r, \vartheta) = J_n(\alpha, \beta, r)exp(jm\vartheta) \tag{1.5}$$

Here, n, m are integers. The kernel function of JFM is orthogonal onto unit disk,

$$\int_0^{2\pi} \int_0^1 P_{nm}(r, \vartheta)P_{kl}(r, \vartheta)rdrd\vartheta = \delta_{nk}\delta_{ml} \tag{1.6}$$

where $\delta_{nk}\delta_{ml}$ are Kronecker deltas and $r = 1$ is the maximum scale of object in the concrete scene. As $exp(jm\theta)$ is orthogonal that is why the radial function $J_n(\alpha, \beta, r)$ must be orthogonal in the interval $[0, 1]$:

$$\int_0^1 J_n(r, \alpha, \beta)J_k(r, \alpha, \beta)rdr = \delta_{nk}(\alpha, \beta) \tag{1.7}$$

Table 1.1: Moments, abbreviations and references

Moments	**Abbreviations**	**References**
Jacobi Fourier Moments	JFM	[15]
Pseudo-Jacobi Fourier Moments	PJFM	[16]
Zernike Moments	ZM	[17]
Pseudo-Zernike Moments	PZM	[18]
Legendre Moments	LM	[19]
Gegenbauer Moments	GM	[20]
Chebyshev Fourier Moments	CFM	[21]
Orthogonal Fourier Mellin Moments	OFMM	[3]
Laguerre Moments	LaM	[22]
Gaussian Hermite Moments	GHM	[23]
Continuous Hahn Moments	CHM	[24]
Bessel Fourier Moments	BFM	[25]
Radial Harmonic Fourier Moments	RHFM	[26]

Jacobi polynomial is expressed as [111]:

$$G_n(\alpha,\beta,r) = \frac{n!(\beta-1)!}{(\alpha+n-1)!}\sum_{s=0}^{n}(-1)^s \times \frac{(\alpha+n+s-1)!}{(n-s)!s!(\beta+s-1)!}r^s \tag{1.8}$$

The Jacobi polynomial in equation (1.8) is also orthogonal in the interval $[0,1]$:

$$\int_0^1 G_n(\alpha,\beta,r)G_m(\alpha,\beta,r)w(\alpha,\beta,r)dr = b_n(\alpha,\beta)\delta_{nm} \tag{1.9}$$

here $w(\alpha,\beta,r)$ is weight function and b_n refers to normalization constant which is given as below:

$$b_n = \frac{n![(\beta-1)!]^2(\alpha-\beta+n)!}{(\beta+n-1)!(\alpha+n-1)!(\alpha+2n)} \tag{1.10}$$

and the weight function is expressed as:

$$w(\alpha,\beta,r) = (1-r)^{\alpha-\beta}r^{\beta-1} \qquad \alpha-\beta>-1, \beta>0 \tag{1.11}$$

In all the above formulae, α and β are real valued parameters. By having different values, they are able to form different types of Jacobi polynomials which are known

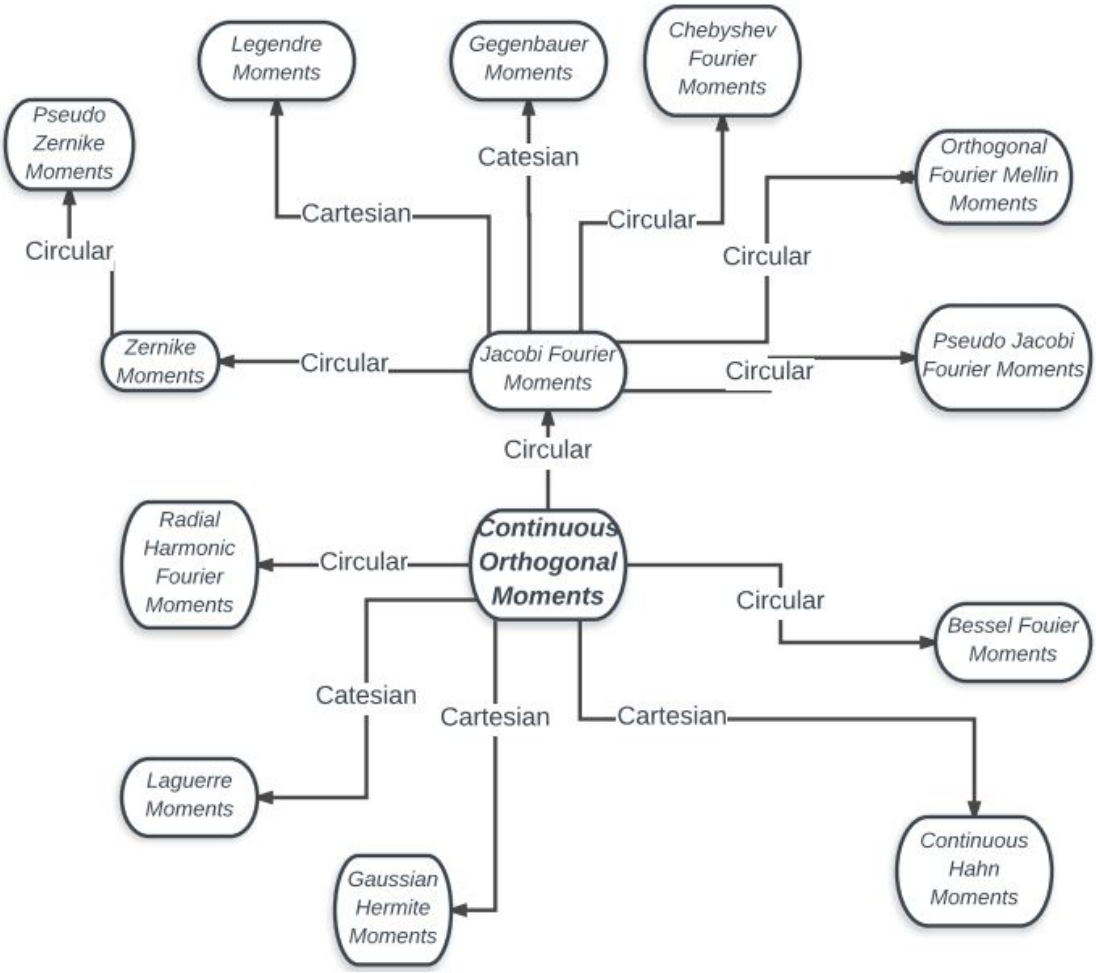

Figure 1.7: Classification of various continuous orthogonal moments

to be special cases of Jacobi polynomials. After comparing equations (1.7) and (1.8), the radial function set is:

$$J_n(\alpha, \beta, r) = \sqrt{\frac{w(\alpha, \beta, r)}{b(\alpha, \beta)r}} G_n(\alpha, \beta, r) \tag{1.12}$$

An image function can be decomposed into superposition of weighted orthogonal components in polar coordinate system as follows:

$$f(r, \vartheta) = \sum_{n=0}^{\infty} \sum_{m=-\infty}^{\infty} \phi_{nm} J_n(r) e^{jm\vartheta} \tag{1.13}$$

here ϕ_{nm} are the coefficients of decomposition and are referred to as Jacobi Fourier Moments:

$$\phi_{nm} = \int_0^{2\pi} \int_0^1 f(r, \vartheta) J_n(\alpha, \beta, r) e^{-jm\vartheta} r dr d\vartheta \tag{1.14}$$

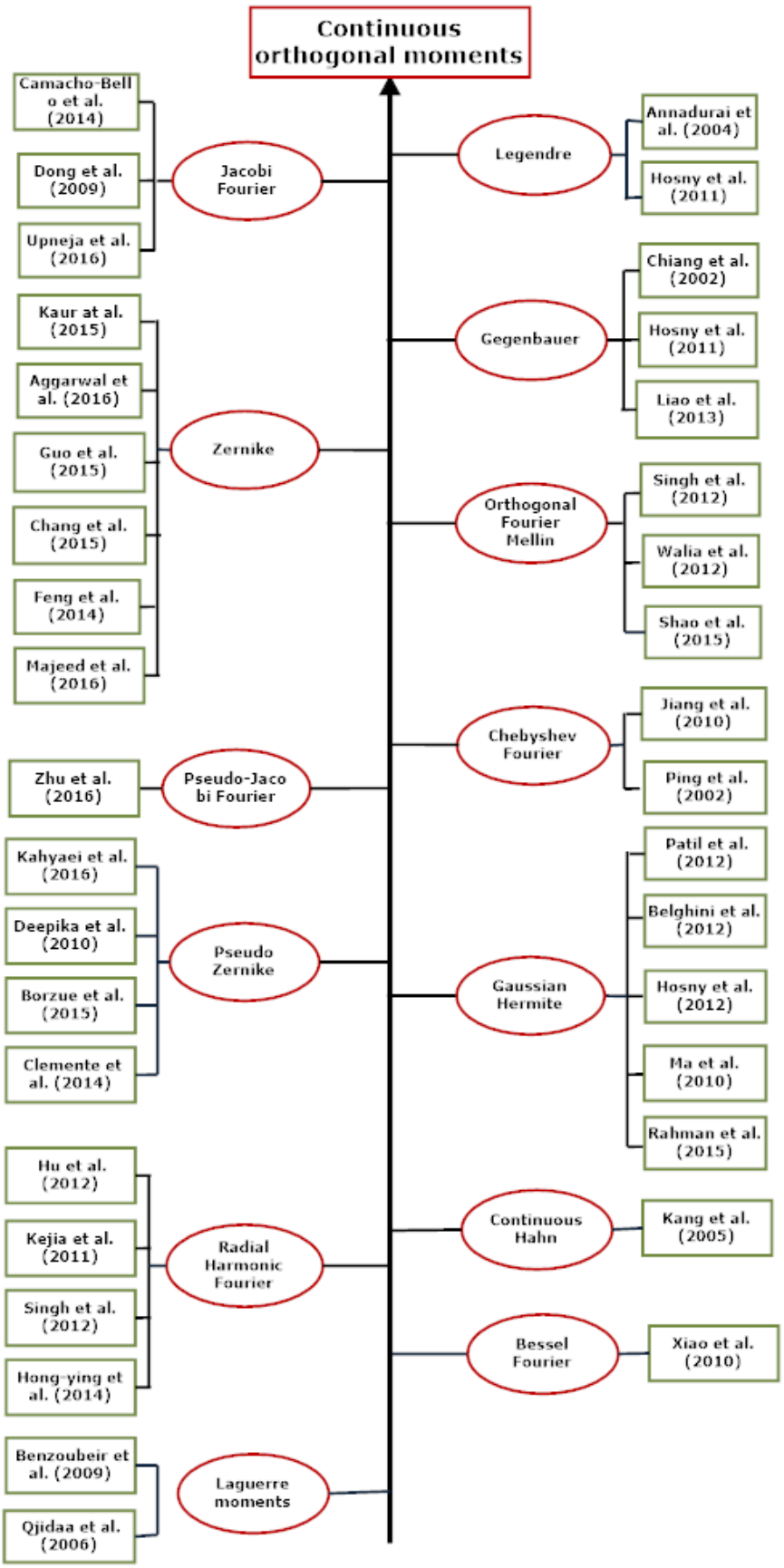

Figure 1.8: Moments and recent literature

1.1.2 Pseudo-Jacobi Fourier Moments

For image $I(r,\theta)$ having order x and repetition y, PJFM over a unit disk are expressed as [16]:

$$P_{xy} = \int_0^{2\pi} \int_0^1 J_x(r) exp(-jy\theta) I(r,\theta) r dr d\theta \tag{1.15}$$

where $J_x(r)$ is real valued Pseudo-Jacobi Fourier radial polynomials given by:

$$J_x(r) = \left[\frac{2(x+2)(r-r^2)}{(x+3)(x+1)}\right]^{\frac{1}{2}} \sum_{k=0}^{n} \frac{(-1)^{x+k}(x+k+3)!}{k!(x-k)!(k+2)!} r^k \tag{1.16}$$

1.1.3 Zernike Moments

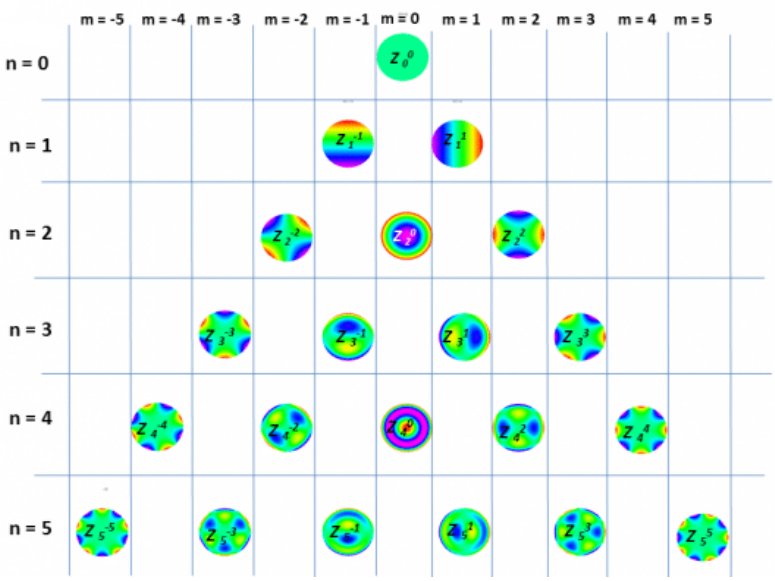

Figure 1.9: First 21 Zernike polynomials

Frits Zernike invented a system of polynomials which are orthogonal onto a unit disk and are known as zernike polynomials [112]. The kernel of ZM consists of a group of orthogonal complex zernike polynomials which are defined inside a unit disk over polar coordinate space. Figure (1.9) shows the first 21 Zernike polynomials where n is order of moment and m is repetition. They are vertically ordered as per radial degree and horizontally according to azimuthal degree. According to [1], if $f(r,\theta)$ represents an image function, p is order with repetition q then two dimensional Zernike Moments can be written as (1.17):

$$Z_{pq} = \frac{p+1}{\pi} \int_0^{2\pi} \int_0^1 f(r,\theta) V_{pq}^*(r,\theta) r dr d\theta \tag{1.17}$$

where $V^*_{pq}(r,\theta)$ is the complex conjugate of zernike polynomials V_{pq} and is given as:

$$V_{pq}(r,\theta) = R_{pq}(r)e^{jq\theta} \tag{1.18}$$

Here $p \geq 0$, $0 \leq \mid q \mid \leq p$, $p- \mid q \mid$ = even, $j = \sqrt{-1}$ and $\theta = \arctan(y/x)$

Radial Polynomials are defined as (1.19):

$$R_{pq}(r) = \sum_{0}^{(p-|q|)/2} (-1)^k \times \frac{(p-k)!}{k!(\frac{p+|q|}{2}-k)!(\frac{p-|q|}{2}-k)!} r^{p-2k} \tag{1.19}$$

Radial polynomials satisfy orthogonality relation as given below (1.20):

$$\int_0^1 R_{pq}(r)R_{p'q}rdr = \frac{1}{2(p+1)}\delta_{pp'} \tag{1.20}$$

where δ_{ij} is known as Kronecker delta. Zernike Polynomials make complete orthogonal set within unit disk, given as (1.21):

$$\int_0^{2\pi}\int_0^1 V_{pq}(r,\theta)V^*_{p'q'}(r,\theta)rdrd\theta = \frac{\pi}{p+1}\delta_{pp'}\delta_{qq'} \tag{1.21}$$

1.1.4 Pseudo-Zernike Moments

The kernel of Pseudo-Zernike Moments (PZM) are made from Pseudo-Zernike polynomials whose basis functions form a complete set of orthogonal functions over the unit disk. They are explained as follows [2]:

$$V_{pq}(r,\theta) = R_{pq}(r)e^{iq\theta} \tag{1.22}$$

where $p \geq 0$, $0 \leq \mid q \mid \leq p$. As per [2], the radial Pseudo-Zernike polynomial $(R_{pq}(r))$ is defined as (1.23):

$$R_{pq}(r) = \sum_{s=0}^{(p-|q|)} \frac{(-1)^s(2p+1-s)!r^{p-s}}{s!(p- \mid q \mid +1-s)!(p- \mid q \mid -s)!} \tag{1.23}$$

For an image $f(r,\theta)$, Pseudo-Zernike Moments are (PZ_{pq}) are defined as (1.24):

$$PZ_{pq} = \frac{p+1}{\pi} \int_0^{2\pi} \int_0^1 f(r,\theta) V_{pq}^*(r,\theta) r dr d\theta \tag{1.24}$$

where $V_{pq}^*(r,\theta)$ is the complex conjugate for $V_{pq}(r,\theta)$. The orthogonality relation of PZM is similar to ZM which is defined as in equation (1.20) and (1.21) for $p = p_{max}$, and the total number of PZM are $(1+p_{max})^2$.

1.1.5 Legendre Moments

Legendre Moments (LM) are derived from the legendre polynomials which are orthogonal over the interval [-1,1] [113]. They are defined on Cartesian coordinate space. Legendre moments can acquire a value near to zero considering redundancy measure, which means independent features of an image can be attained [19]. As described in [1], the basis function of LM is given by equation (1.25):

$$\varphi_{nm}(x,y) = P_m(x) P_n(y) \tag{1.25}$$

where $P_p(x)$ is pth order of Legendre polynomial and the $(n+m)th$ order is given as (1.26):

$$L_{nm} = \frac{(2n+1)(2m+1)}{4} \int_{-1}^{1} \int_{-1}^{1} P_n(x) P_m(y) f(x,y) dx dy \tag{1.26}$$

where $P_n(x)$ is n^{th} order of Legendre polynomial which is given in (1.27):

$$P_n(x) = \frac{1}{2^n} \sum_{k=0}^{\frac{n}{2}} (-1)^k \times \frac{(2n-2k)!}{k!(n-k)!(n-2k)!} x^{n-2k} \tag{1.27}$$

1.1.6 Gegenbauer Moments

Gegenbauer polynomials, also known as Ultraspherical polynomials are a set of polynomials which are orthogonal over interval $[-1,1]$. Gegenbauer polynomials of order n are defined with a scaling parameter $\alpha > -0.5$ as [114] below:

$$G_n^{\alpha}(x) = \frac{(2\alpha)_n}{n!} \left[{}_2F_1\left(-n, 2\alpha+1+n; \alpha+\frac{1}{2}; \frac{1-x}{2} \right) \right] \tag{1.28}$$

where ${}_2F_1$ is a hypergeometric function defined as:

$$ {}_2F_1(a,b;c;z) = \sum_{k=0}^{\infty} \frac{a_k b_k}{c_k} \frac{z^k}{k!} \tag{1.29} $$

α_k is Pochhammer symbol expressed as:

$$ \alpha_k = \alpha(\alpha+1)(\alpha+2),...,(\alpha+k-1) \tag{1.30} $$

Gegenbauer polynomial of order n is defined more explicitly as:

$$ G_n^{\alpha}(x) = \sum_{k=0}^{\lfloor \frac{n}{2} \rfloor} B_{n,k}^{\alpha} x^{n-2k} \tag{1.31} $$

Coefficient matrix $B_{n,k}^{\alpha}$ is defined as:

$$ B_{n,k}^{\alpha} = (-1)^k \frac{\Gamma(n-k+\alpha)2^{n-2k}}{k!(n-2k)!\Gamma(\alpha)} \tag{1.32} $$

where $\Gamma(.)$ is a gamma function and $\lfloor \frac{n}{2} \rfloor$ is floor function which is either equal to $\frac{n-1}{2}$ or $\frac{n}{2}$ for odd and even values of n respectively. Gegenbauer polynomials are orthogonal over a square $[-1,1] \times [-1,1]$ and they satisfy the following orthogonality property:

$$ \int_{-1}^{1} G_n^{\alpha} x) G_m^{\alpha}(x) w^{\alpha}(x) dx = C_n(\alpha)\delta_{mn} \tag{1.33} $$

with following weight function:

$$ w^{\alpha}(x) = (1-x^2)^{(\alpha 0.5)} \tag{1.34} $$

here δ_{nm} is Kronecker delta and the normalization constant $C_n(\alpha)$ is stated as:

$$ C_n(\alpha) = \frac{2\pi\Gamma(n+2\alpha)}{2^{2\alpha} n!(n+\alpha)[\Gamma(\alpha)]^2} \tag{1.35} $$

Gegenbauer polynomials obey the following recursive relation:

$$ G_{n+1}^{\alpha}(x) = \frac{2n+\alpha}{n+\alpha} x G_n^{\alpha}(x) - \frac{(n+2\alpha-1)}{n+1} G_{n-1}^{\alpha}(x) \tag{1.36} $$

where $G_0^\alpha(x) = 1, G_1^\alpha(x) = 2\alpha x$ and $n \geq 1$. So, orthogonal Gegenbauer Moments of order n with repetition m are expressed as:

$$A_{n,m} = \frac{1}{C_n(\alpha)C_m(\alpha)} \int_{-1}^{1}\int_{-1}^{1} f(x,y)G_n^\alpha(x)G_m^\alpha(y)w^\alpha(x)w^\alpha(y)dxdy \tag{1.37}$$

where n and m are non-negative integers.

Equation (1.37) is approximated by [115, 116] to provide the discrete version of the image as follows:

$$\tilde{A}_{nm} = \frac{1}{C_n(\alpha)C_m(\alpha)} \frac{4}{MN} \sum_{i=1}^{M}\sum_{j=1}^{N} G_n^\alpha(x_i)G_m^\alpha(y_j)w^\alpha(x_i)w^\alpha(y_j)f(x_i,y_j) \tag{1.38}$$

1.1.7 Chebyshev Fourier Moments

CFM [64] of order x and repetition y in polar coordinates for image $I(r,\theta)$ are defined inside unit circle as:

$$A_{xy} = \int_0^{2\pi}\int_0^1 C_x(r)exp(-jy\theta)I(r,\theta)rdrd\theta \tag{1.39}$$

where $C_x(r)$ are real valued Chebyshev Fourier Radial polynomials expressed as:

$$C_x(r) = \left[\frac{64(1-r)}{\pi^2 r}\right]^{\frac{1}{4}} \sum_{k=0}^{\frac{x+2}{2}} \frac{(-1)^k(x-k)!}{k!(x-2k)!}(4r-2)^{n-2k} \tag{1.40}$$

1.1.8 Orthogonal Fourier Mellin Moments

Sheng and Shen [3] introduced Orthogonal Fourier Mellin Moments in year 1994. OFMM are based on radial polynomials and they are defined in polar coordinate system with order p and repetition q as below:

$$O_{pq} = \frac{1}{2\pi a_p} \int_0^{2p}\int_0^1 f(r,\theta)Q_p(r)e^{-iq\theta}rdrd\theta \tag{1.41}$$

where

$$Q_p(r) = \sum_{k=0}^{p} \alpha_{pk} r^k \tag{1.42}$$

here

$$\alpha_{pk} = (-1)^{p+k}\frac{(p+k+1)!}{(p-k)!k!(k+1)!} \tag{1.43}$$

where $p \geq 0, q = 0, \pm 1, \pm 2, ...$ and $0 \leq r \leq 1$. The set $Q_p(r)$ is orthogonal over the interval $0 \leq r \leq 1$.

1.1.9 Laguerre Moments

Laguerre Polynomials are the basis for Laguerre Moments. For an image function $I(x, y)$, if $l_n^{\alpha}(x)$ is a set of discrete orthogonal polynomials and $e^{-x}x^{\alpha}$ is weight which satifies the following condition:

$$\sum_{x=0}^{N-1} e^{-x}x^{\alpha}L_m(x)L_n(x) = \rho(n, N)\delta_{mn} \tag{1.44}$$

where $m \geq 0$ and $n \leq N - 1$, then the coefficient moments L_{mn} are defined as:

$$L_{mn} = \frac{1}{\rho(p, N)\rho(q, N)} \sum_{x=0}^{N-1}\sum_{y=0}^{N-1} e^{-x}x^{\alpha}L_p(x)L_q(y)I(x, y) \tag{1.45}$$

where $p, q = 0, 1, 2, ..., N - 1$ and $\rho(p, N)$ is given by:

$$\rho(p, N) = \sum_{x=0}^{N-1} e^{-x}x^{x}L_p(x)^2 \tag{1.46}$$

The discrete Laguerre polynomials are expressed as [117]:

$$L_n^{\alpha}(x) = \frac{(\alpha + 1)_n}{n!}[{}_1F_1(-n; \alpha + 1; x)] \tag{1.47}$$

where $\alpha > -1$ and $n, x, y = 0, 1, 2, 3, ..., N - 1$. ${}_1F_1(.)$ is generalized hyper geometric function and is given by:

$${}_1F_{1(\alpha;\gamma;x)} = 1 + \sum_{v=1}^{\infty} \frac{\alpha(\alpha + 1)...(\alpha + v - 1)}{\gamma(\gamma - 1)...(\gamma + v - 1)v!} \tag{1.48}$$

Papers [118, 119, 120] shows the continuous form of Laguerre Moments and their applications.

1.1.10 Gaussian-Hermite Moments

GHM are derived from Hermite polynomials which are defined over domain $(-\infty, \infty)$ and have degree m are [4, 5]:

$$H_m = (-1)^m exp(x^2) \frac{d^m}{dx^m} exp(-x^2) \tag{1.49}$$

it exists the recursive calculation: $H_m(x) = 2xH_{m-1}(x) - 2(m-1)H_{m-2}(x)$ with initial conditions $H_0(x) = 1$ and $H_1(x) = 2x$. $H_m(x)$ is orthogonally: $\int_{-\infty}^{\infty} exp(-x^2) H_m(x) H_n(x) dx = 2^m m! \sqrt{\pi} \delta_{mn}$, here $exp(-x^2)$ is weight function. It can be seen that Hermite base function is neither zero nor more smoothed at window edges. So, it brings window infection for analyzing signal. To solve this problem, Gaussian Hermite polynomials were introduced. As per equation (1.49), normalized Hermite polynomials are defined as:

$$\hat{H}_m(x) = \frac{1}{\sqrt{2^m m! \sqrt{\pi}}} e^{-x^2/2} H_m(x) \tag{1.50}$$

it gives $\int_{-\infty}^{\infty} \hat{H}_m(x) \hat{H}_n(x) dx = \delta_{mn}$. Normalized Hermite polynomials with standard deviation of Gaussian function are expressed as:

$$\hat{H}_m(x/\sigma) = \frac{1}{\sqrt{2^m m! \sqrt{\pi} \sigma}} e^{-x^2/2\sigma^2} H_m(x/\sigma) \tag{1.51}$$

Gaussian Hermite functions are more smoothed at window edges than other moments and also less sensitive to noise. Therefore, they can facilitate image recognition. For image function f(x,y), GHM are defined as:

$$G_{m,n} = \int_{-\infty}^{\infty} \int_{-\infty}^{\infty} f(x,y) \hat{H}_m(x/\sigma) \hat{H}_n(y/\sigma) dx dy \tag{1.52}$$

basis function of degree $m+n$ is :

$$\varphi_{m,n}(x,y) = \hat{H}_m(\frac{x}{\sigma}) \hat{H}_n(\frac{y}{\sigma}) = \frac{1}{\sqrt{2^{m+n-1} m! n!}} G(x,y,\sigma) H_m(x/\sigma) H_n(y/\sigma) \tag{1.53}$$

1.1.11 Continuous Hahn Moments

CHM are derived from continuous Hahn polynomials which were introduced by Askey and Wilson [121]. The Continuous Hahn polynomials are defined as:

$$P_n(x;\alpha,\beta) = i^n \left[{}_3F_2 \left(\begin{matrix} -n, n+2\alpha+2\beta-1, \beta-ix \\ \alpha+\beta, 2\beta \end{matrix} ; 1 \right) \right] \tag{1.54}$$

These polynomials are orthogonal w.r.t positive absolutely continuous weight function given by:

$$W(x) = (\mid \Gamma(\alpha + ix)\Gamma(\beta + ix) \mid)^2 \tag{1.55}$$

here $-\infty < x < \infty$ and $\alpha, \beta > 0$ or $\alpha = \overline{\beta}$ and $Re\alpha > 0$.

1.1.12 Bessel Fourier Moments

BFM are derived from Bessel function of first kind which is defined as [114, 122]:

$$J_v(x) = \sum_{i=0}^{\infty} \frac{(-1)^i}{i!\Gamma(v+i+1)} \left(\frac{x}{2}\right)^{v+2i} = \frac{(x/2)}{\Gamma(v+1)}({}_0F_1(v+1, -(x/2)^2)) \tag{1.56}$$

here v is real constant, $\Gamma(a)$ is gamma function and ${}_0F_1$ is generalized hypergeometric function. Bessel function is solution of below equation (1.57):

$$y" + \frac{1}{x}y' + (1 - v^2/x^2)y = 0 \tag{1.57}$$

It has following recurrence relation [123]:

$$J_{v-1}(x) + Jv + 1(x) = \frac{2v}{x}J_v(x) \tag{1.58}$$

BFM in polar coordinates are defined as:

$$B_{nm} = \frac{1}{2\pi z_n} \int_0^{2\pi} \int_0^1 f(r,\theta) J_v(\lambda_n r) e^{-jm\theta} r dr d\theta \tag{1.59}$$

here $f(r,\theta)$ is image, $n = 0, 1, 2, 3, ...$ and $m = 0, \pm 1, \pm 2, \pm 3, ...$ is moment order, $z_n = \frac{(J_{v+1}(\lambda_n))^2}{2}$ is normalization constant, $J_v(\lambda_n r)$ is Bessel polynomial in r of degree n and λ_n is nth zero of $J_v(r)$. $J_v(\lambda_n r)$ is orthogonal over range [0,1].

$$\int_0^1 r J_v(\lambda_n r) J_v(\lambda_i) dr = a_n \delta_{ni} \tag{1.60}$$

here $\delta_n i$ is Kronecker delta. The basis function of the BFM is orthogonal over unit disk.

$$\int_0^1 \int_0^{2\pi} [J_v(\lambda_n r) e^{-jp\theta}]^* J_v(\lambda_m r) e^{-jp\theta} r dr d\theta = 2\pi z_n \delta_{nm} \delta_{pq} \tag{1.61}$$

1.1.13 Radial Harmonic Fourier Moments

Haiping Ren in 2003 proposed the Radial Harmonic Fourier Moments (RHFM) [26] and found them better than other ways of describing images. For an image function $I(r,\theta)$, RHFM H_{mn} of order $m \geq 0$ with repetition $\mid n \mid \geq 0$ in polar coordinates are defined as:

$$H_{mn} = \frac{1}{2\pi} \int_0^{2\pi} \int_0^1 I(r,\theta) V_{mn}^*(r,\theta) r dr d\theta \tag{1.62}$$

here $V_{mn}^*(r,\theta)$ is complex conjugate of kernel function $V_{mn}(r,\theta)$, which is expressed as:

$$V_{mn}(r,\theta) = R_m(r) e^{jn\theta} \tag{1.63}$$

Radial kernel function of RHFM is a sinusoidal function in r stated as:

$$R_m(r) = \begin{cases} \frac{1}{\sqrt{r}}, & m = 0 \\ \sqrt{\frac{2}{r}} \cos(\pi m r), & m = even \\ \sqrt{\frac{2}{r}} \sin(\pi(m+1)r), & m = odd \end{cases} \tag{1.64}$$

Kernel function of RHFM is orthogonal over unit disk and satisfies the following condition:

$$\int_0^{2\pi} \int_0^1 V_{mn}(r,\theta) V_{mn}^*(r,\theta) r dr d\theta = 2\pi \delta_{mm'} \delta_{nn'} \tag{1.65}$$

where δ is Kronecker symbol such that $\delta_{ij} = 1$ for $i = j$ and otherwise $\delta_{ij} = 0$. For maximum order, m_{max} and repetition n_{max}, total number of RHFM are $(1 + m_{max})(1 + 2n_{max})$.

1.2 Thesis Organization

This thesis is organized as follows:

- **Chapter 1**: This chapter introduces the moments, continuous orthogonal moments with their formulae, plant diseases, existing ways of detecting diseases in plants. This chapter also identified the prominent research gaps. Further, research objectives are defined with the research methodology used in this study.
- **Chapter 2**: This chapter covers the maximum research done in the field of plant disease recognition using various techniques. The techniques used recently for the disease recognition includes k-nearest neighbor, Gaussian

distribution, histogram of template features, CNN, SIFT features and bag of visual words. Fractional-order orthogonal moments are also discussed in which conversion of simple integer order moments to fractional-order orthogonal moments is shown.

- **Chapter 3**: This chapter includes research gaps, problem statement and contribution. It states the problem and its background that this thesis is solving. The contribution to solve the problem is presented in points.
- **Chapter 4**: This chapter focuses on the proposed fractional-order Zernike moments and the outer mapping approach used in the calculation which is better than inner square to circle mapping. Graphs between radial Zernike polynomials and values of r at different values of α are also shown. Algorithm of the whole recognition process and block diagram are also shown and discussed. Feature selection and SVM classifier are also defined in this section.
- **Chapter 5**: This chapter includes database description, image preprocessing ways and performance metric. The results obtained after experimentation are discussed and the graph representing those reults is also drawn. Database sample and image preprocessing process is presented with the help of a diagram. Image preprocessing includes resizing, conversion to gray scale and normalization. The performance metric used is recogntion rate whose calculation procedure is also shown.
- **Chapter 6**: This chapter concludes the work done in this thesis. Future research work that can be done related to this area is also discussed here.

Chapter 2

Literature Review

Below is the work done by various authors in the field of plant disease detection and recognition using different techniques.

In [124], authors have used deep learning and convolutional neural network for detecting the plant leaf diseases. A deep CNN is trained that can differentiate among healthy plant, plant with diseases and the surrounding images. Dataset is prepared from internet by downloading images from different sources and consists of total 33469 images.

[125] proposes an image segmentation algorithm that can automatically detect and classify the diseases present in the plant leaves. Image segmentation is done with the help of genetic algorithm. Comparison of SVM and neural network classifier is shown considering classification of plant species such as beans, cotton, guava, lemon and mango. A new technique involving SVM classifier, genetic algorithm, and neural network is introduced for the development of a computer based vision system for identification of plant species automatically.

In [126], the techniques for identification of three types of diseases such as leaf rust, berry disease and wilt disease which are present on the leaf part of Ethiopian coffee plant are presented. Comparative analysis of four classifiers such as artificial neural network, naive, k-nearest neighbor and a hybrid of radial basis function and self-organizing map is shown. Five different segmentation techniques are used in experimentation which are FCM, K-means, Gaussian distribution, Otsu and the combination of K-means and Gaussian distribution. The combination of K-means and Gaussian distribution and the hybrid classifier approach is found to be better than other methods with an accuracy of 92.1%.

Banana leaves are prone to various diseases such as yellow sigatoka, black sigatoka, panama wilt, bunchy top and streak virus. So, to distinguish these diseases and suggesting a medicine for removal of each disease, [127] have proposed a software solution with the use of image processing methods. Color and Histogram of Template (HOT) features are extracted from leaf images and artificial neural network is used for disease identification and grading the amount of disease present. As per the severity of an identified disease, a particular pesticide or medicine with its

amount is suggested by the system.

In [128], authors have made a graphical user interface for detecting the type of leaf disease and the percentage of affected area. Neural network and Naive Bayes classifiers performance in evaluating the percentage of the region affected by the diseases is compared considering different type of diseases. Three feature extractions from binary masks of the leaves are performed such as finescale margin feature histogram, centroid contour distance curve shape signature and by an interior texture feature histogram.

In [129], plant disease identification model is introduced with the use of convolutional neural networks which can distinguish between healthy leaves and thirteen diseases of different plants. The images taken for implementation are healthy leaf images, background images and the images having diseased leaves of pear, peach, apple, pair and grapevine. After experimentation, the proposed technique found to be efficient and obtained the precision around 93%.

[130] proposes a new technique for identifying and classifying the various diseases that affect the paddy plant such as brown spot disease, leaf blast disease and bacterial blight disease. The two major steps involved are paddy plant disease detection and the detected disease recognition. Disease detection is done using Haar-like features and AdaBoost classifier and obtained accuracy is 83.33%. The recognition of diseases is performed with the use of scale invariant feature transform (SIFT) features, K-nearest neighbor classifier and support vector machine. The recognition rate using SVM is 91.10% and using K-nearest neighbor is 93.33%.

In [131] a multi-classification approach based upon two stage SVM is proposed. The first classifier S1 considers color moments (mean, standard deviation and skewness) for each RGB and HSV spaces to calculate 18 color features (3*3+3*3=18). The second SVM classifier S2 considers gray level co-occurrence matrix (GCLM) [132] for texture features (energy, contrast, entropy, homogeneity, correlation) to obtain 30 features for each HSV and RGB (5*3+5*3=30). Eleven shape features (area, perimeter, circularity, solidity, extent, major/minor axis lengths, diameter, eccentricity, centroid) are also extracted from the binary image. This method first classifies the leaves based upon color (yellow/white versus black/browns) and then based upon their textures to find out 6 leaf diseases using multi classification (Leaf nimers, Thrips, Tuta absoluta, Powdery mildew, Early blight, Late blight) and has average correct classification accuracy of 87.8%.

In [133] singular value decomposition (SVD) based feature extraction and data representation is used for cucumber disease recognition. Watershed algorithm is used to segment the spot image and then divided into blocks for local and global

SVD values are extracted from each of them. Then SVM is used to classify three types of leaf cucumber diseases. In [129] convolutional neural network (CNN) based approach is used to classify 13 types of leaf diseases using Caffe, a framework developed by Berkely Vision and Learning Center which is able to achieve a considerable precision value.

In [134] Fractional Krawtchouk Transform (FrKT) using the eigenvalues and eigen vectors decomposition scheme to obtain a general form of Krawtchouk Transform through watermarking example are proposed. Fractional orders are adjusted for FrKT robustness and watermarking performance. Another approach based on fractional order orthogonal moments is studied in [14] which can be represented in Cartesian and polar coordinates through shifted Legendre polynomials. It has been shown in this study that fractional order moments perform better for face recognition, image reconstruction and region of interest feature extraction.

In [135] sparse representation classification is performed for cucumber leaf disease detection. Image segmentation is done through K-means followed by color and shape feature extraction. Sparse representation enhances the performance and computational costs. It has 85.7% recognition rate to detect seven types of cucumber diseases. Soybean disease detection is studied in [136] with average time of 0.1 second per image. It is based upon local descriptors and Bag of Visual words which is a summarization technique. Three diseases are classified out of 1200 images and this technique can be extended to other crops as well.

Chapter 3

Problem Statement

3.1 Research Gaps

In most state of art techniques, the plant diseases are analyzed manually by an expert. Most part of the disease present in a plant reflects on its leaves. So, plant infection can be easily detected from leaves. However, it takes too much time for an expert to analyze each leaf carefully and detect its malady. So, there is a need to propose a technique which can quickly detect plant ailment and whether the plant is healthy or not just by analyzing the leaf images. As per the reviewed literature, various techniques used recently for disease recognition present on plant leaves includes k-nearest neighbor, Gaussian distribution, histogram of template features, CNN, SIFT features and bag of visual words. These techniques capture redundant features from leaf images which consequently affects the output generated through the classifier and the disease maynot be recognized correctly or a leaf may be classified as a different disease label. Orthogonal moments can be used in place of above techniques for the recognition process. They are rotation, scaling and translation invariant and also show very less information redundancy which is useful in classifying leaves into correct classes. They are not used in this area before. Moreover, orthogonal moments can also be modified from integer-order moments to fractional-order moments which can give better results.

3.2 Statement

To overcome the above limitations, a new technique is proposed for recognition of ailments present in plants. The new proposed technique is fractional-order ZM which is an improved version of Zernike moments that comes under continuous orthogonal moments. FZM has the fractional order and ZM is of integer type order. In this study, grape leaves are chosen for classification into four classes which are healthy, eska, black rot and leaf blight with the use of FZM and SVM classifier. After prerocessing, FZM are extracted from leaf images which are then selected with the help of random forest. Feature matrix of images after feature

selection is put into the SVM classifier for classification of images into respective classes.

3.3 Contribution

- Introduction to fractional-order Zernike moments that results in better feature extraction compared to integer order Zernike moments and other feature extraction methods. Fractional order moments are capable to capture more feature details compared to integer order moments as proved in [14].
- Application of continuous orthogonal moments to plant disease detection is proposed. Orthogonal moments are more efficient than other approaches because they show minimum information redundancy in feature extraction. Moreover proposed fractional-order orthogonal moments are improved version of orthogonal moments.
- To automate the detection of plant leaf diseases without the need of an expert which is more efficient and faster framework to recognize diseases.

Chapter 4

Proposed Methodology

Figure (4.1) shows the block diagram of the whole process of plant disease recognition. Firstly, in the training phase, each image from the inputted plant leaf image database is preprocessed which includes resizing of image, conversion to gray scale and normalization. After preprocessing, fractional order Zernike moments of images are calculated and the training feature matrix is obtained. This training data is put into SVM classifier to train it so that it will be able to recognize the various types of plant diseases in future. Now in the testing phase, when an image comes for prediction of disease, it will be prepocessed in the same way as training phase. Then the FZM are extracted and feature selection is performed to get the final feature vector for test image. This feature vector is put into the trained classifier which will find whether the plant is healthy or not and if not, then the disease present in plant will be identified. Algorithm (4.1) shows the complete pseudo code for the calculation of FZM. In this, variable A has the actual magnitudes of moments that act as features of input images.

4.1 Fractional-order Zernike moments

This is a new feature extraction technique introduced here. Image feature extraction means finding those unique and distinctive values that describe an image in a reduced form and are able to distinguish the image from other images. In this study, the unique values related to the images are fractional-order Zernike moments which act as distinctive features to recognize the leaf diseases. These moments involve minimum information redundancy and are invariant to rotation , scaling, orientation and translation. The difference between FZM and existing ZM lies in the order. Table (4.1) shows the notations or symbols used for variables in the experiments and their explanation.

The definition FZM is almost similar to the ZM with replacement of integer-order with the fractional order. There are two types of square to circle mapping used by various authors to map pixel coordinates onto a unit circular disk. The two mapping techniques are inner circle mapping and outer circle mapping. In inner

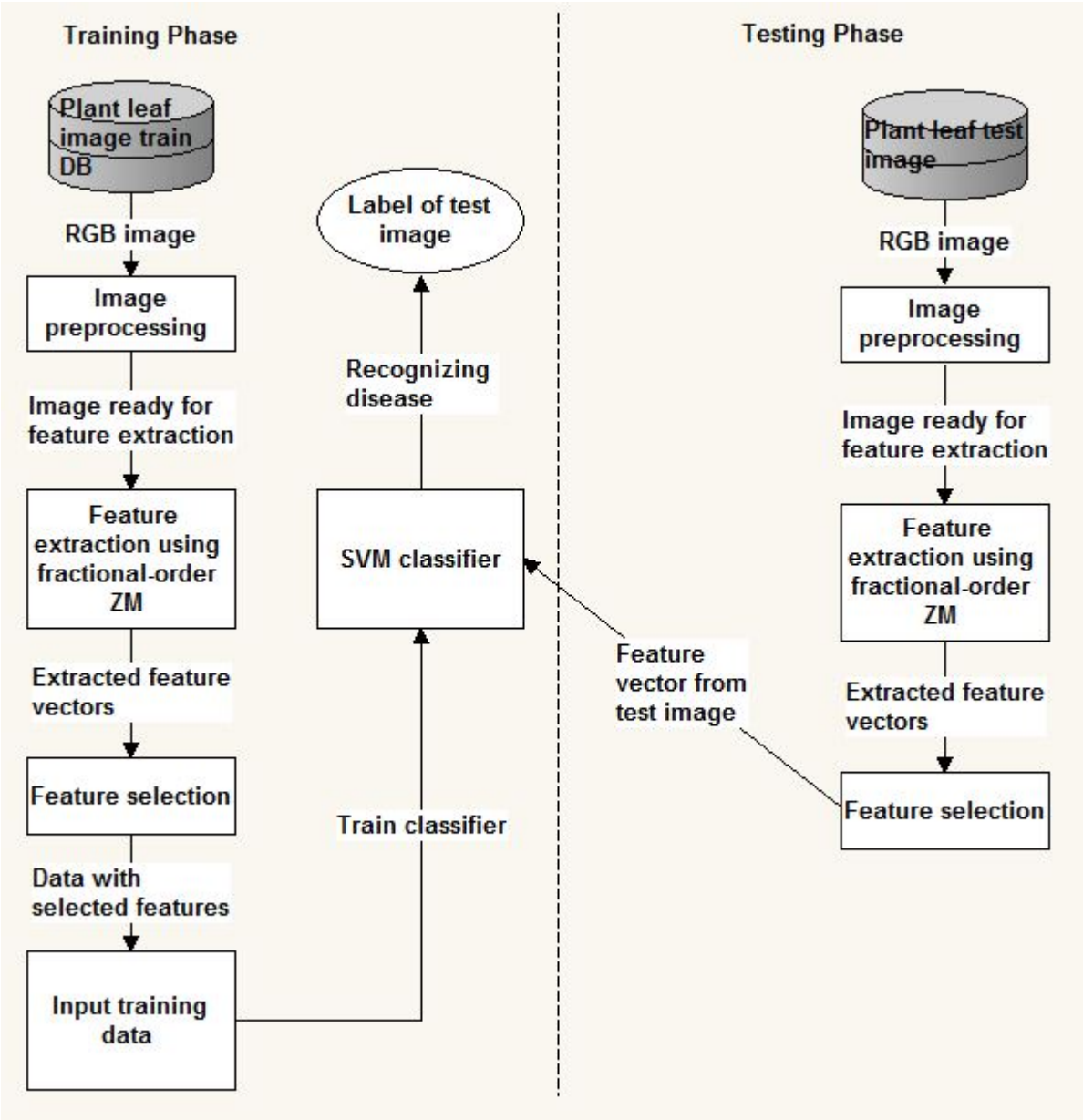

Figure 4.1: Block diagram for plant leaf disease recognition

circle mapping technique, an image is mapped onto a unit circular disk in such a way that the center of image is transformed into origin and pixel coordinates of image are normalized within a range of unit disk. In this mapping, corner pixels are not included in moments computation, so there is a loss of information which is a disadvantage. Outer circle mapping overcomes the drawback of inner circle mapping approach. In this, the whole image is mapped inside the unit circular disk, so there is no pixel loss while calculation of moments. In figure (4.2), (a) shows the inner circle mapping and (b) shows outer circle mapping technique. It can be seen in the figure that there will be different values of radius r in both the techniques which consequently change the calculation of FZM. Outer mapping technique is used here due to its advantage of no pixel loss.

Algorithm 4.1 Plant disease recognition algorithm

File ← All types of leaf images
NoI ← length of *File*; *Size* ← 50
for $k \in \{1, \ldots, NoI\}$ **do**
  image ← *imread(File(k).name))*
  Images(:,:,k) ← *double(rgb2gray(imresize(image,[size size])))*
  f(:,:,k) ← *mat2gray(Images(:,:,k))*
end for
order ← *20 or 30*
x,y ← *1:size*
$[X, Y] \leftarrow meshgrid(x, y)$
$X \leftarrow X - 1$; $Y \leftarrow Y - 1$
Calculate values of x_i and y_j using equations (4.9) and (4.10) respectively
$R \leftarrow \sqrt{(x^2 + y^2)}$; $\theta = \arctan(y_j, x_i)$
for $k \in \{1, \ldots, NoI\}$ **do**
  count ← 1
  for $p \in \{0, \ldots, order\}$ **do**
    for $q \in \{0, \ldots, p\}$ **do**
      if $(p - \mid q \mid)\%2) \neq 0$ **then**
        continue
      end if
      $\alpha \leftarrow 0.5, 1, 1.5, 2, 2.5$ (one value at a time)
      Calculate value of radial polynomials ($B_{pq}(\alpha, r)$) using using equation (4.2) and then fractional Zernike polynomials ($A_{pq}(r, \theta)$) using equation (4.1)
      Now Using equation (4.13), calculate the value of FZM
      $A(count, k) \leftarrow abs(FZM)$
      $count \leftarrow count + 1$
    end for
  end for
end for
End

Fractional-order Zernike polynomials are a set of orthogonal polynomials that are defined inside unit circle, i.e., $x^2 + y^2 = 1$. They are defined as (4.1):

$$A_{pq}(r, \theta) = A_{pq}(x, y) = B_{pq}(\alpha, r)e^{iq\theta} \tag{4.1}$$

where p can be zero or a positive integer such that $p \geq 0$ and q can be positive or negative integer satisfying the constraints, $0 \leq \mid q \mid \leq p$, $p - \mid q \mid$ = even, $i = \sqrt{-1}$ and r represents the length of vector from origin to pixel (x, y). The angle θ represents the angle between r vector and x-axis in the counter clockwise direction which is given as $\theta = \arctan(y/x)$ and B_{pq} is the radial polynomial which

Table 4.1: Variables and definitions

Variable	**Definition**
F_{pq}	Fractional order Zernike Moments
A_{pq}	Fractional order Zernike polynomials
A_{pq}	Complex conjugate of fractional order Zernike polynomials
$B_{p,q}$	Radial polynomials
$I(x, y)$	Image function
δ_{ab}	Kronecker delta
α	Real number used for making integer order fractional
p	Moment order
q	Repetition
r	Length of vector from origin to (x, y)
D	Diameter of circle on which image is mapped
N	Dimension of image
x_i, y_i	Mapped pixel coordinates

is defined in equation (4.2):

$$B_{pq}(\alpha, r) = \sqrt{\alpha} \sum_{k=0}^{(p-|q|)/2} (-1)^k \times \frac{(p-k)!}{k!(\frac{p+|q|}{2}-k)!(\frac{p-|q|}{2}-k)!} r^{\alpha(p-2k)+(\alpha-2)/2} \tag{4.2}$$

where $\alpha \in R^+$. From equation (4.5) and (4.2), it can be derived that order of FZM is $q + \alpha p + (\alpha - 2)/2$.

Figures (4.3, 4.4, 4.5, 4.6 and 4.7) show the plots of fractional-order radial Zernike polynomials at different values of α which are drawn to check the numerical stability of the polynomials. The values of α are chosen as per stability of polynomials to obatain more accurate results. X-axis is r values and Y-axis represent the values of $B_{pq}(\alpha, r)$. It can be seen in the figures that roots of fractional-order radial Zernike polynomials are gathered in interval close to 0 when $\alpha < 1$ and in interval near 1 when $\alpha > 1$. Also, the order of fractional-order radial shifted Zernike polynomials is $\alpha p + (\alpha - 2)/2 < n$ when $\alpha < 1$. Fractional-order radial Zernike polynomials with $\alpha < 2$ are becoming large when r is tending to 0 which may result in numerical instability. So, FZM with $\alpha > 2$ are able to provide efficient results.

The equation showing the satisfaction of orthogonality relation by fractional Zernike

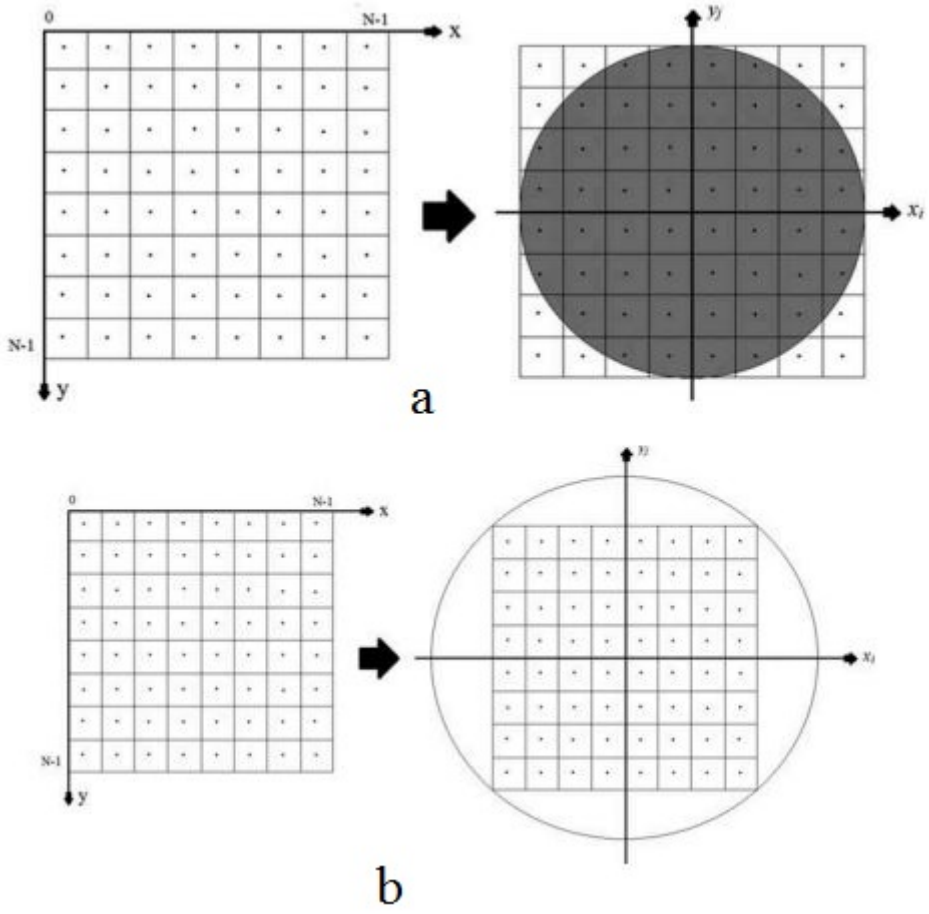

Figure 4.2: Inner and outer circle mapping techniques

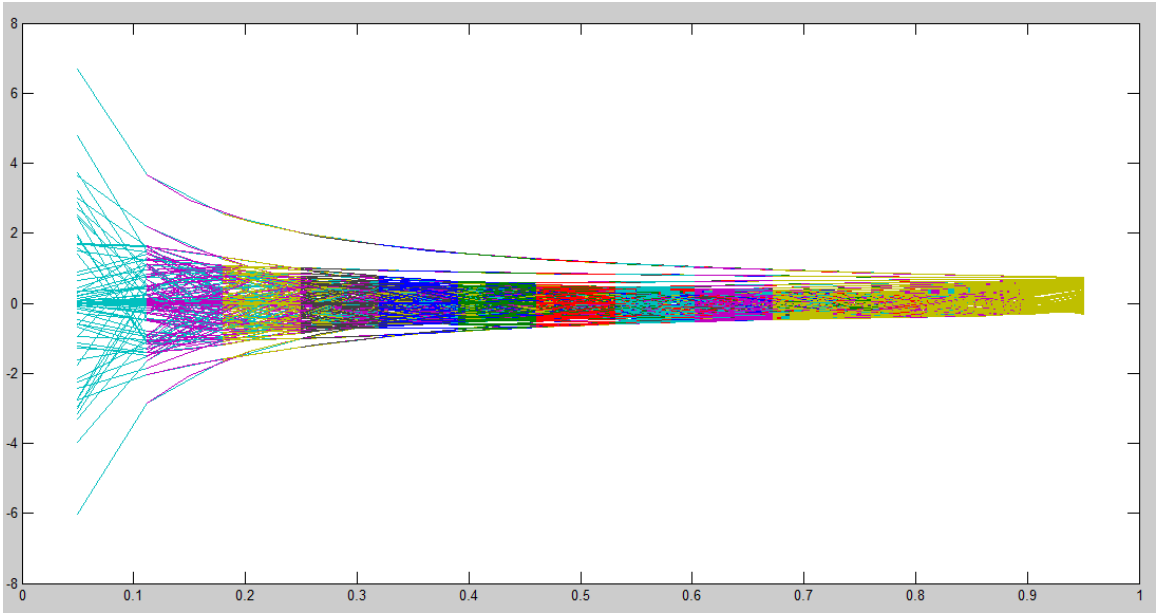

Figure 4.3: Plot between r values and $B_{pq}(\alpha, r)$ radial polynomials at $\alpha = 0.5$

polynomials is given below:

$$\int_0^{2\pi} \int_0^1 A^*_{pq}(x,y) A_{p'q'}(x,y) dxdy = \frac{\pi}{p+1} \delta_{pp'} \delta_{qq'} \tag{4.3}$$

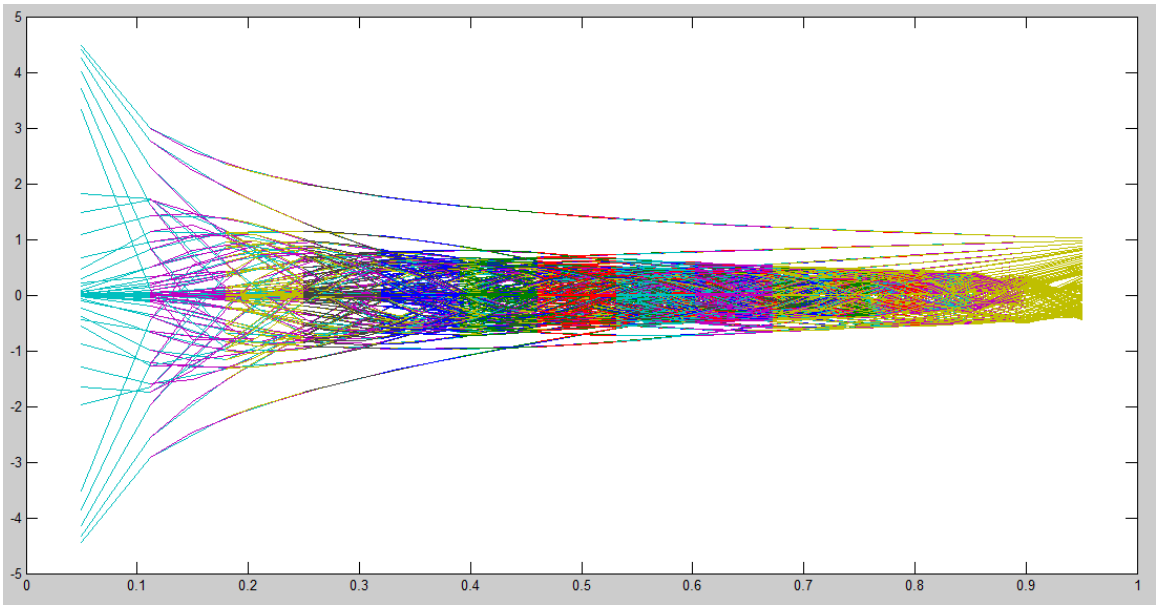

Figure 4.4: Plot between r values and $B_{pq}(\alpha, r)$ radial polynomials at $\alpha = 1$

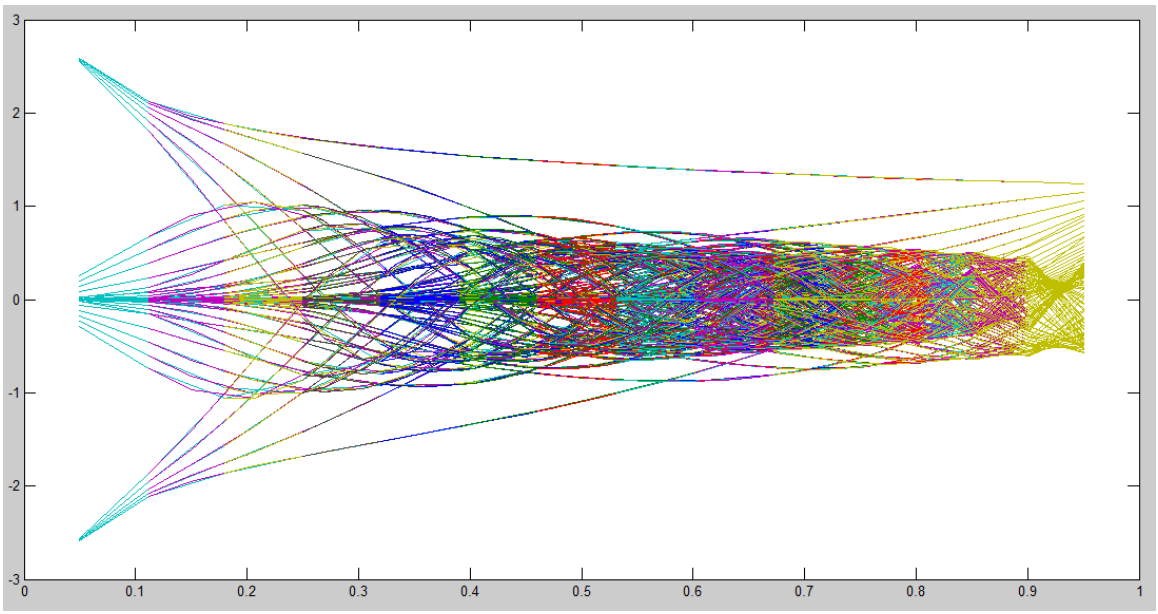

Figure 4.5: Plot between r values and $B_{pq}(\alpha, r)$ radial polynomials at $\alpha = 1.5$

here, $A^*_{pq}(x, y)$ represents the complex conjugate and δ_{ab} is Kronecker delta which is expressed as:

$$\delta_{ab} = \begin{cases} 1, & a = b \\ \\ 0, & otherwise \end{cases} \tag{4.4}$$

FZM are extracted from the image by projecting it onto complex orthogonal fractional Zernike polynomials. For an image function $I(r, \theta)$, fractional-order ZM are

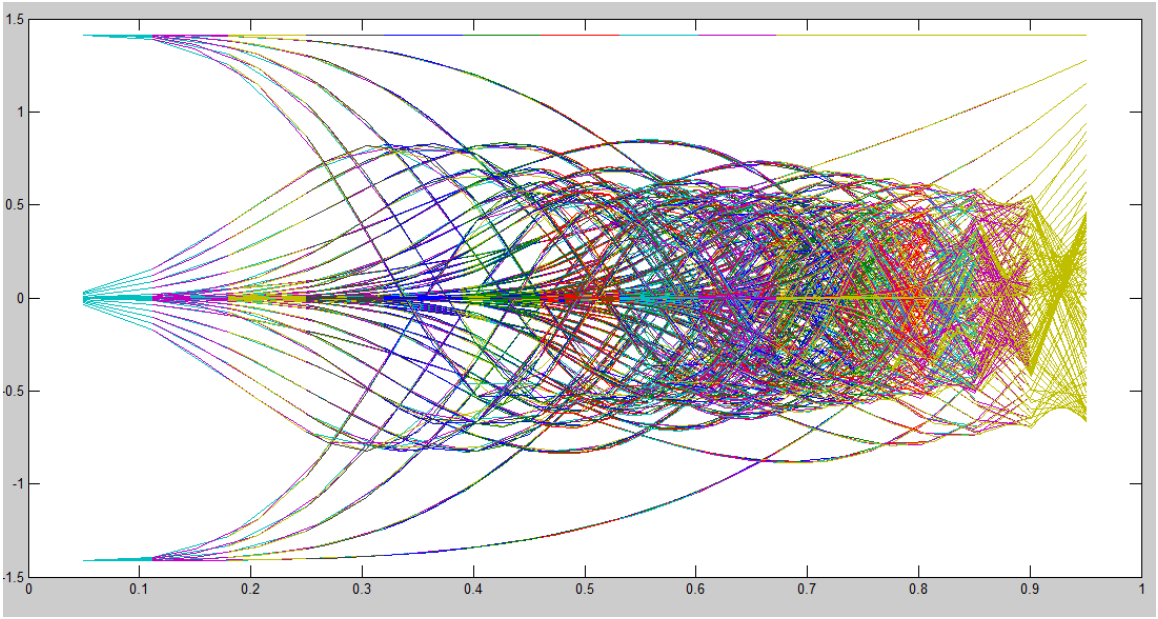

Figure 4.6: Plot between r values and $B_{pq}(\alpha, r)$ radial polynomials at $\alpha = 2$

defined as:

$$F_{pq} = \frac{p+1}{\pi} \int_0^{2\pi} \int_0^1 I(r,\theta) A^*_{pq}(r,\theta) r dr d\theta \tag{4.5}$$

$$= \frac{p+1}{\pi} \int \int_{x^2+y^2 \leq 1} I(x,y) A^*_{pq}(x,y) dx dy \tag{4.6}$$

The integrals are replaced by summations for a digital image. So, equation (4.6) becomes:

$$F_{pq} = \frac{p+1}{\pi} \sum_x \sum_y I(x,y) A^*_{pq}(x,y) \Delta x \Delta y \tag{4.7}$$

If I(x,y) is a digital image of size N x N then FZM is given as:

$$F_{pq} = \frac{p+1}{\pi} \sum_0^{N-1} \sum_0^{N-1} I(x_i,y_i) A^*_{pq}(x_i,y_i) \Delta x_i \Delta y_i \tag{4.8}$$

With center of pixel (i, j), (x_i, y_i) are the mapped pixel coordinates that occupies the area of $[x_i - \Delta x/2, x_i + \Delta x/2] \times [y_j - \Delta y/2, y_j + \Delta y/2]$ and [33] are defined as equations (4.9) and (4.10):

$$x_i = \frac{2i + 1 - N}{D} \tag{4.9}$$

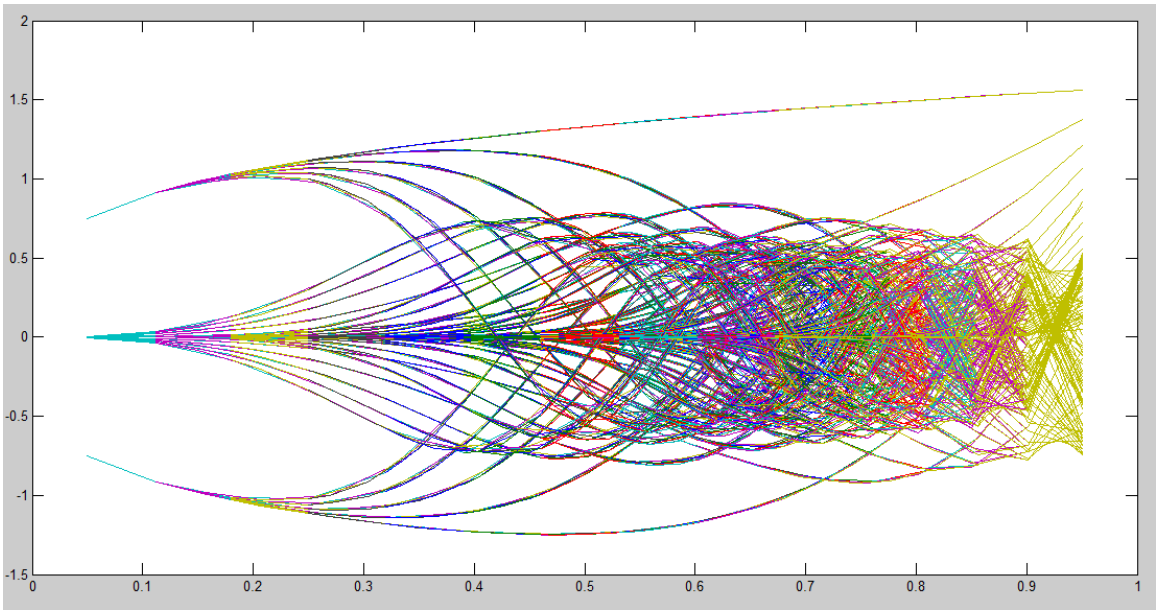

Figure 4.7: Plot between r values and $B_{pq}(\alpha, r)$ radial polynomials at $\alpha = 2.5$

$$y_j = \frac{2j + 1 - N}{D} \tag{4.10}$$

where Δx and Δy can be expressed as:

$$\Delta x_i = \Delta y_j = \frac{2}{D} \tag{4.11}$$

Using equations (4.9, 4.10) and (4.11), equation (4.8) can be written as:

$$F_{pq} = \frac{4(p+1)}{\pi D^2} \sum_{0}^{N-1} \sum_{0}^{N-1} I(x_i, y_i) A^*_{pq}(x_i, y_i) \tag{4.12}$$

Here, the value of D should be chosen as per the mapping technique. For inner circle mapping, the value of D will be N and for outer circle mapping approach, it will be $N\sqrt{2}$, which can also be visualized in the figure (4.2). For inner circle mapping, FZM can be calculated using equation (4.12) just by replacing D with N. However, in outer circle mapping, FZM can be calculated as:

$$F_{pq} = \frac{2(p+1)}{\pi N^2} \sum_{0}^{N-1} \sum_{0}^{N-1} I(x_i, y_i) A^*_{pq}(x_i, y_i) \tag{4.13}$$

Like ZM, the square to circle mapping makes the magnitudes of FZM as rotation and scale invariant. So, the magnitudes of FZM act as image representing features.

4.2 Feature selection

The term feature selection means selection of significant features or attributes from the extracted features for constructing a model. In this process, the non-essential features are left and the features that highly affect the model training and its testing accuracy are chosen. Feature selection is done to simplify the model, shorten training data, remove redundant features and overfitting. In this paper, feature importance is measured using Random Forest classifier and then the first fifty features are picked for model training in case of order 20 and first 150 features are chosen in case of order 30. The effect of feature selection can be seen in the results shown in table (5.1). Accuracy has been improved comparative to results obtained without feature selection.

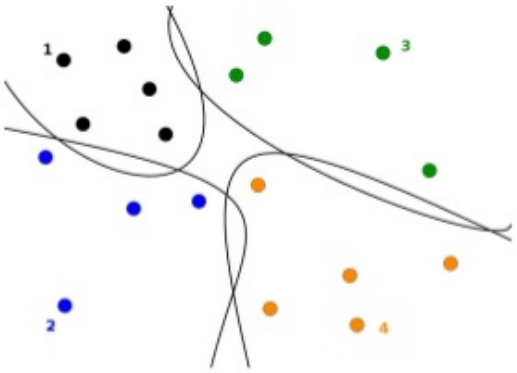

Figure 4.8: Example classification of 4 classes of data using SVM

4.3 Support Vector Machine

Support Vector Machine (SVM) is a machine learning model which comes under supervised learning approach. Its concept was given by *Vapnik* and *Chervonenkis* in 1963. It is used for classification of data into two or more classes, regression and outlier detection. Binary classification SVM tutorial can be found in [137] and multi-classification SVM operational details are in [138]. Figure (4.8) shows an example of multiclass SVM. There is a separating hyperplane in SVM which separates data into class labels. Hyperplane plays an important role in good separation of data points. It effectively separate data points with a decision boundary which lies at the maximum distance from respective classes which means right in the middle. This is because greater is the margin, lower the generalization error of a model for testing. SVM has various kernel functions available depending

upon the underlying data distribution such as linear, radial basis function and polynomial, quadratic. In linear kernels, the hyperplane should be a straight line, however, in non-linear kernel functions the boundary that separates data points is not a straight line. So, non-linear kernel SVM are much powerful than linear kernels because they can capture more complex relationships between data for classification. However, non-linear SVM takes more time to train as it is computationally intensive. Basically the data is first projected into a higher dimensional feature space using the kernel function where it is linearly separable. Afterwards, when the decision boundary is projected back into original data space, it results into a non-linear hyperplane. Here we are using radial basis function (rbf) SVM for classification of grape leaf diseases. SVM gives better results in case where number of data dimensions is larger than the number of samples in data and it also consumes less memory.

Chapter 5

Experimental Results

For experimentation, 400 images are collected consisting of 100 images from each of the four classes such as healthy, black rot, eska and leaf blight depicted as $1, 2, 3$ and 4 respectively in the train database. After preprocessing, gray scale normalized images of pixel size 50 x 50 are obtained. Then ZM and FZM are extracted from each image which provide a feature vector of a particular size depending upon the selected order of ZM and FZM respectively. In this paper, two orders 20 and 30 are used for implementation. The number of moments (NoM) retrieved as per given order p can be calculated as (5.1):

$$NoM = \begin{cases} \frac{1}{4}(p+1)(p+3), & p = odd \\ \\ \frac{1}{4}(p+2)^2, & p = even \end{cases} \tag{5.1}$$

So, as per equation (5.1), the number of moments retrieved are 121 and 256 on order 20 and 30 respectively. Then a feature matrix is obtained after combining feature vectors of each image. Firstly, the SVM classifier is trained and tested using this feature matrix to obtain the classifier accuracy. Then the feature selection is done on this feature matrix and process is repeated. The results obtained using ZM and FZM at different values of α and with or without feature selection are shown in table (5.1). These results are also shown in the form of a bar graph to have a visual comparison in figure (5.7). It can be seen in table (5.1) that FZM with $\alpha = 2.5$ has the maximum recognition rate of 95.12%.

5.1 Database description

Images are downloaded one by one from Plant Village website to make the whole grape leaf database. The whole image repository is fully described in [139]. Grape leaf is mainly affected by diseases such as black rot, eska (black measles or spanish measles) and leaf blight (isariopsis leaf spot) which are considered in this study. The images of disease affected leaves and a healthy grape leaf are shown in figures (5.1, 5.2, 5.3 and 5.4). So, grape leaves are recognized as of four categories: healthy,

Figure 5.1: Healthy

Figure 5.2: Black rot

Figure 5.3: Esca

Figure 5.4: Leaf blight

black rot, eska and leaf blight. A total of 400 images are taken for experimentation consisting of 100 images from each mentioned category. Images are of same as well as different sizes. However, all the images are re-sized to 50 x 50 pixels for efficient calculation of results and then used for implementation.

5.2 Image preprocessing

Image preprocessing is a very crucial step of image recognition process as it increases the accuracy and make the proposed technique more efficient. The goal of preprocessing is to improve the image data, getting better feature extraction,

Figure 5.5: Sample image database for disease classification. First row corresponds to healthy leaves. Second, third and forth rows corresponds to Black rot, esca, leaf blight diseases.

gaining consistency and also improves some image features important for additional processing. In this paper three steps are performed under preprocessing stage: (a) image resizing, (b) conversion of image from RGB to gray scale, (c) normalization. After image preprocessing step, images will have better feature extraction capability as they contain only useful information now. Preprocessing steps are defined below:

- **Resize**: The collected images are all of different sizes having different number of pixels. So, in order to get accurate results, image resizing has an important role. All the collected images are resized to 50 x 50 pixels which make them square in shape and of same size. Moreover, the computation process is also fasten up as the size is decreased. Figure (5.6) shows the resized image obtained from the original image.

- **Conversion**: Conversion of images from RGB scale to gray scale is also necessary as it increases speed of processing, decreases code complexity and gray images can be easily visualized. Third image in figure (5.6) shows the gray scale image of its previous image.

- **Normalization**: The images of plant leaves are captured in different sizes and from different distances. The size may change because of illumination variations. Such changes in the images will influence the plant disease recognition results. So, it is necessary to compensate for such changes or deformations for achieving more accurate results. Linear normalization (I_n) of

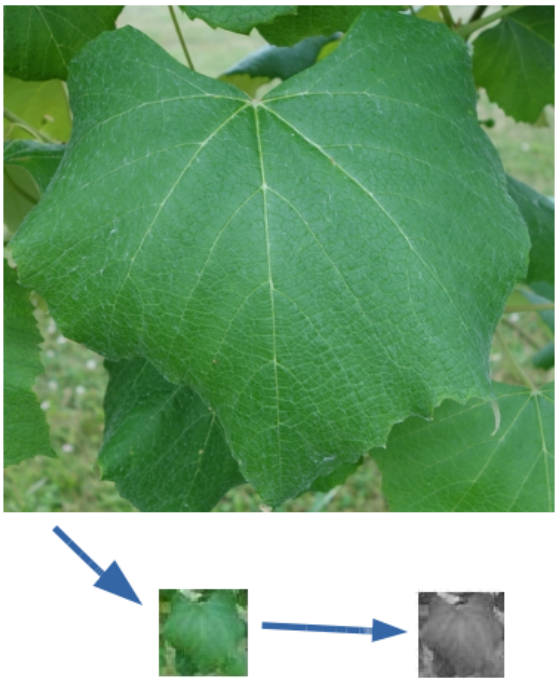

Figure 5.6: Image resize to 50 × 50 and gray scale conversion for FZM input to extract features

a gray scale image can be calculated as (5.2) where Min and Max are minimum and maximum intensity values of image and $newMin$ and $newMax$ are the new intensity values.

$$I_n = (I - Min)\frac{newMax - newMin}{Max - Min} + newMin \tag{5.2}$$

5.3 Performance metric

The performance metric used for comparison between moments is recognition rate (RR). It represents the percentage of all the test data objects that have been classified into the correct class by the classifier. It can be expressed as:

$$RR = \begin{cases} 1, & if \quad Actual = Predicted \\ \\ 0, & if \quad Actual \neq Predicted \end{cases} \tag{5.3}$$

Final value of recognition rate ($in\%$) can be obtained by taking mean of the value got in equation (5.3) and calculating its percentage.

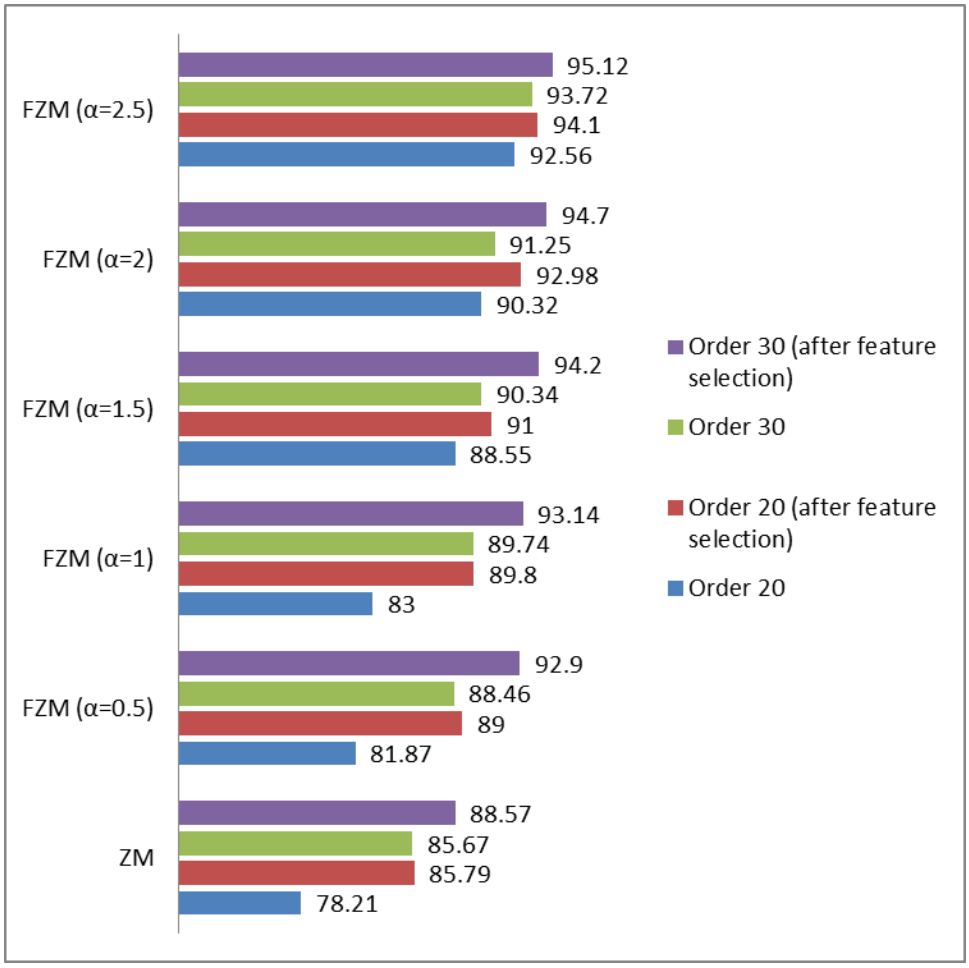

Figure 5.7: Recognition rate (RR) comparison of plant disease detection using integer and fractional order Zernike moments. α determines the value of fractional order for FZM

Table 5.1: Recognition rates (in %) of moments with and without feature selection

Moments	**Order 20**	**Order 20 (after feature selection)**	**Order 30**	**Order 30 (after feature selection)**
ZM	78.21	85.79	85.67	88.57
FZM (α=0.5)	81.87	89	88.46	92.9
FZM (α=1)	83	89.8	89.74	93.14
FZM (α=1.5)	88.55	91	90.34	94.2
FZM (α=2)	90.32	92.98	91.25	94.7
FZM (α=2.5)	92.56	94.1	93.72	95.12

Chapter 6

Conclusion and Future Work

In this thesis, a new version of continuous orthogonal Zernike moments is introduced which is known as fractional Zernike moments. Fractional Zernike moments are used to extract features and then SVM is used for plant disease detection. The plant leaf chosen for study is grape which suffers from three major diseases and can be recognized as belonging to one of the four classes: healthy, black rot, eska and leaf blight. Comparison of ZM and FZM at different values of α and also with and without feature selection is shown on the basis of recognition rate of class labels. After experimentation, it is found that FZM provides more promising results compared to ZM at all values of α. However, the highest recognition rate obtained is 95.12% using FZM at $order = 30$ (after feature selection) and $\alpha = 2.5$.

Future extension of this work could be to analyze the proposed approach for image reconstruction, character or face recognition, iris identification and image watermarking. Other classifiers can be incorporated such as artificial neural network, k-nearest neighbour, decision tree and random forest. Moreover continuous and discrete orthogonal moments can also be made fractional and applied for image processing.

References

[1] Michael Reed Teague. Image analysis via the general theory of moments∗. *J. Opt. Soc. Am.*, 70(8):920–930, Aug 1980.

[2] C-H Teh and Roland T. Chin. On image analysis by the methods of moments. *IEEE Transactions on pattern analysis and machine intelligence*, 10(4):496–513, 1988.

[3] Yunlong Sheng and Lixin Shen. Orthogonal fourier–mellin moments for invariant pattern recognition. *JOSA A*, 11(6):1748–1757, 1994.

[4] Jun Shen, Wei Shen, and Danfei Shen. On geometric and orthogonal moments. *International Journal of Pattern Recognition and Artificial Intelligence*, 14(07):875–894, 2000.

[5] Youfu Wu and Jun Shen. Properties of orthogonal gaussian-hermite moments and their applications. *EURASIP Journal on Advances in Signal Processing*, 2005(4):439420, 2005.

[6] Huazhong Shu, Limin Luo, and Jean-louis Caatrieux. Moment-based approaches in imaging. 1. basic features [a look at...]. *IEEE Engineering in Medicine and Biology Magazine*, 26(5):70–74, 2007.

[7] Jan Flusser, Barbara Zitova, and Tomas Suk. *Moments and moment invariants in pattern recognition*. John Wiley & Sons, 2009.

[8] Ying-Han Pang. Enhanced pseudo zernike moments in face recognition. *IEICE Electronics Express*, 2(3):70–75, 2005.

[9] Xiang-Yang Wang, E-No Miao, and Hong-Ying Yang. A new svm-based image watermarking using gaussian–hermite moments. *Applied Soft Computing*, 12(2):887–903, 2012.

[10] S Sharma Ashok, M Patel Mitul, and P Chaudhari Jitendra. Palm print identification using zernike moments.

[11] EM Arvacheh and HR Tizhoosh. Pattern analysis using zernike moments. In *Instrumentation and Measurement Technology Conference, 2005. IMTC 2005. Proceedings of the IEEE*, volume 2, pages 1574–1578. IEEE, 2005.

[12] Chandan Singh, S Pooja, and Rahul Upneja. On image reconstruction, numerical stability, and invariance of orthogonal radial moments and radial harmonic transforms. *Pattern recognition and image analysis*, 21(4):663–676, 2011.

[13] Chao Kan and Mandyam D Srinath. Invariant character recognition with zernike and orthogonal fourier–mellin moments. *Pattern recognition*,

35(1):143–154, 2002.

[14] Bin Xiao, Linping Li, Yu Li, Weisheng Li, and Guoyin Wang. Image analysis by fractional-order orthogonal moments. *Information Sciences*, 382:135–149, 2017.

[15] Ziliang Ping, Haiping Ren, Jian Zou, Yunlong Sheng, and Wurigen Bo. Generic orthogonal moments: Jacobi–fourier moments for invariant image description. *Pattern Recognition*, 40(4):1245–1254, 2007.

[16] Guleng Amu, Surong Hasi, Xingyu Yang, and Ziliang Ping. Image analysis by pseudo-jacobi (p= 4, q= 3)–fourier moments. *Applied optics*, 43(10):2093–2101, 2004.

[17] Hasan Abdel Qader, Abdul Rahman Ramli, and Syed Al-Haddad. Fingerprint recognition using zernike moments. *Int. Arab J. Inf. Technol.*, 4(4):372–376, 2007.

[18] A Nabatchian, E Abdel-Raheem, and M Ahmadi. Human face recognition using different moment invariants: A comparative study. In *Image and Signal Processing, 2008. CISP'08. Congress on*, volume 3, pages 661–666. IEEE, 2008.

[19] S Annadurai and A Saradha. Face recognition using legendre moments. In *ICVGIP*, pages 461–466, 2004.

[20] Simon Liao and Jing Chen. Object recognition with lower order gegenbauer moments. *Lecture Notes on Software Engineering*, 1(4):387, 2013.

[21] Hongqing Zhu, Yan Yang, Zhiguo Gui, Yu Zhu, and Zhihua Chen. Image analysis by generalized chebyshev–fourier and generalized pseudo-jacobi–fourier moments. *Pattern Recognition*, 51:1–11, 2016.

[22] Hassan Qjidaa. Image reconstruction by laguerre moments. In *Proceedings of the Second International Symposium on Communication, Control and Signal Processing ISCCSP*, volume 6, 2006.

[23] Youfu Wu and Jing Wu. Recognizing moving objects based on gaussian-hermite moments and art neural networks. *Journal of Convergence Information Technology*, 5(8):63–70, 2010.

[24] H Koelink. On jacobi and continuous hahn polynomials. *Proceedings of the American Mathematical Society*, 124(3):887–898, 1996.

[25] Bin Xiao, Jian-Feng Ma, and Xuan Wang. Image analysis by bessel–fourier moments. *Pattern Recognition*, 43(8):2620–2629, 2010.

[26] Haiping Ren, Ziliang Ping, Wurigen Bo, Wenkai Wu, and Yunlong Sheng. Multidistortion-invariant image recognition with radial harmonic fourier moments. *JOSA A*, 20(4):631–637, 2003.

[27] Jia-li Dong, Guo-rui Yin, and Zi-liang Ping. Geometrically robust image watermarking based on jacobi-fourier moments. *Optoelectronics Letters*, 5:387–

390, 2009.

[28] NVS Sree, Rathna Lakshmi, and C Manoharan. An automated system for classification of micro calcification in mammogram based on jacobi moments. *International Journal of Computer Theory and Engineering*, 3(3):431, 2011.

[29] Rahul Upneja. Accurate and fast jacobi-fourier moments for invariant image recognition. *Optik-International Journal for Light and Electron Optics*, 127(19):7925–7940, 2016.

[30] C Camacho-Bello, C Toxqui-Quitl, A Padilla-Vivanco, and JJ Báez-Rojas. High-precision and fast computation of jacobi–fourier moments for image description. *JOSA A*, 31(1):124–134, 2014.

[31] V Subbiah Bharathi and L Ganesan. Orthogonal moments based texture analysis of ct liver images. *Pattern Recognition Letters*, 29(13):1868–1872, 2008.

[32] Ashutosh Aggarwal and Karamjeet Singh. Zernike moments-based retrieval of ct and mr images. In *India Conference (INDICON), 2015 Annual IEEE*, pages 1–6. IEEE, 2015.

[33] Ashutosh Aggarwal and Chandan Singh. Zernike moments-based gurumukhi character recognition. *Applied Artificial Intelligence*, 30(5):429–444, 2016.

[34] Tiansheng Wang and Simon Liao. Chinese character recognition by zernike moments. In *Audio, Language and Image Processing (ICALIP), 2014 International Conference on*, pages 771–774. IEEE, 2014.

[35] AJ Nor'aini, P Raveendran, and N Selvanathan. Human face recognition using zernike moments and nearest neighbor classifier. In *Research and Development, 2006. SCOReD 2006. 4th Student Conference on*, pages 120–123. IEEE, 2006.

[36] Guojiang Wang. Facial expression recognition method based on zernike moments and mce based hmm. In *Computational Intelligence and Design (ISCID), 2016 9th International Symposium on*, volume 2, pages 408–411. IEEE, 2016.

[37] Shahbaz Majeed. Face recognition using fusion of local binary pattern and zernike moments. In *Power Electronics, Intelligent Control and Energy Systems (ICPEICES), IEEE International Conference on*, pages 1–5. IEEE, 2016.

[38] Dariusz Frejlichowski. Application of zernike moments to the problem of general shape analysis. *Control and Cybernetics*, 40(2):515–526, 2011.

[39] Ma Xing, Mu Chunyang, Wang Yan, Wang Xiaolong, and Chen Xuetao. Traffic sign detection and recognition using color standardization and zernike moments. In *Control and Decision Conference (CCDC), 2016 Chinese*, pages 5195–5198. IEEE, 2016.

[40] Harman Preet Kaur and Anmol Sharma. Offline handwritten signature verification using zernike moments. In *Computer Vision, Pattern Recognition, Image Processing and Graphics (NCVPRIPG), 2015 Fifth National Conference on*, pages 1–4. IEEE, 2015.

[41] Tang-You Chang, Shen-Chuan Tai, and Guo-Shiang Lin. A near-duplicate video retrieval method based on zernike moments. In *Signal and Information Processing Association Annual Summit and Conference (APSIPA), 2015 Asia-Pacific*, pages 860–864. IEEE, 2015.

[42] Weixing Zhu, Yan Zhu, Xincheng Li, and Dengting Yuan. The posture recognition of pigs based on zernike moments and support vector machines. In *Intelligent Systems and Knowledge Engineering (ISKE), 2015 10th International Conference on*, pages 480–484. IEEE, 2015.

[43] Mohammed Saaidia, Narima Zermi, and Messaoud Ramdani. Facial expression recognition using neural network trained with zernike moments. In *Artificial Intelligence with Applications in Engineering and Technology (ICAIET), 2014 4th International Conference on*, pages 187–192. IEEE, 2014.

[44] Guanyuan Feng, Lin Ma, and Xuezhi Tan. Ground traffic signs recognition based on zernike moments and svm. In *Information Technology and Artificial Intelligence Conference (ITAIC), 2014 IEEE 7th Joint International*, pages 478–481. IEEE, 2014.

[45] Kalpana Sharma, Garima Joshi, and Maitreyee Dutta. Analysis of shape and orientation recognition capability of complex zernike moments for signed gestures. In *Signal Processing and Integrated Networks (SPIN), 2015 2nd International Conference on*, pages 730–735. IEEE, 2015.

[46] Chong-Yaw Wee and Raveendran Paramesran. On the computational aspects of zernike moments. *Image and Vision Computing*, 25(6):967–980, 2007.

[47] George A Papakostas, Yiannis S Boutalis, Dimitris A Karras, and Basil G Mertzios. A new class of zernike moments for computer vision applications. *Information Sciences*, 177(13):2802–2819, 2007.

[48] Yun Guo, Chunping Liu, and Shengrong Gong. Improved algorithm for zernike moments. In *Control, Automation and Information Sciences (ICCAIS), 2015 International Conference on*, pages 307–312. IEEE, 2015.

[49] Chandan Singh and Sukhjeet K Ranade. Image adaptive and high-capacity watermarking system using accurate zernike moments. *IET Image Processing*, 8(7):373–382, 2014.

[50] Javad Haddadnia, Majid Ahmadi, and Karim Faez. An efficient feature extraction method with pseudo-zernike moment in rbf neural network-based

human face recognition system. *EURASIP Journal on Advances in Signal Processing*, 2003(9):267692, 2003.

[51] Ying-Han Pang, TBJ Andrew, NCL David, and FS Hiew. Palmprint verification with moments. 2004.

[52] Sahar Kahyaei and Mohamad-Shahram Moin. Robust matching of fingerprints using pseudo-zernike moments. In *Control, Instrumentation, and Automation (ICCIA), 2016 4th International Conference on*, pages 116–120. IEEE, 2016.

[53] C Lakshmi Deepika, A Kandaswamy, C Vimal, and B Sathish. Invariant feature extraction from fingerprint biometric using pseudo zernike moments. In *Proceedings of the International Joint Journal Conference on Engineering and Technology*, pages 104–108, 2010.

[54] Yongqi ng Xin, Simon Liao, and Miroslaw Pawlak. Geometrically robust image watermarking via pseudo-zernike moments. In *Electrical and Computer Engineering, 2004. Canadian Conference on*, volume 2, pages 939–942. IEEE, 2004.

[55] Mehdi Dehghan and Karim Faez. Farsi handwritten character recognition with moment invariants. In *Digital Signal Processing Proceedings, 1997. DSP 97., 1997 13th International Conference on*, volume 2, pages 507–510. IEEE, 1997.

[56] Carmine Clemente, Luca Pallotta, Ian Proudler, Antonio De Maio, John J Soraghan, and Alfonso Farina. Multi-sensor full-polarimetric sar automatic target recognition using pseudo-zernike moments. In *Radar Conference (Radar), 2014 International*, pages 1–5. IEEE, 2014.

[57] Nasim Borzue and Karim Faez. Object contour detecting using pseudo zernike moment and multi-layer perceptron. In *Biomedical Engineering (ICBME), 2015 22nd Iranian Conference on*, pages 304–308. IEEE, 2015.

[58] Yang Qing-Yue, Gao Fei, and NIE Qing. A modified l-iterative algorithm for fast computation of pseudo-zernike moments. In *2009 2nd International Congress on Image and Signal Processing*, 2009.

[59] Bo Li, Guojun Zhang, and Bo Fu. A novel algorithm for accurate computation of pseudo-zernike moments in cartesian coordinates. In *Computer and Communication Technologies in Agriculture Engineering (CCTAE), 2010 International Conference On*, volume 2, pages 334–337. IEEE, 2010.

[60] Bo Li, Guojun Zhang, and Bo Fu. Accurate computation and error analysis of pseudo-zernike moments. In *Education Technology and Computer (ICETC), 2010 2nd International Conference on*, volume 4, pages V4–85. IEEE, 2010.

[61] GA Papakostas, YS Boutalis, DA Karras, and BG Mertzios. Efficient com-

putation of zernike and pseudo-zernike moments for pattern classification applications. *Pattern Recognition and Image Analysis*, 20(1):56–64, 2010.

[62] Li Bo. Accurate computation of pseudo-zernike moments. In *Wavelet Active Media Technology and Information Processing (ICCWAMTIP), 2015 12th International Computer Conference on*, pages 220–223. IEEE, 2015.

[63] Khalid M Hosny. Image representation using accurate orthogonal gegenbauer moments. *Pattern Recognition Letters*, 32(6):795–804, 2011.

[64] ZiLiang Ping, RiGeng Wu, and YunLong Sheng. Image description with chebyshev–fourier moments. *JOSA A*, 19(9):1748–1754, 2002.

[65] Yongjing Jiang, Ziliang Ping, and Laibin Gao. A fast algorithm for computing chebyshev-fourier moments. In *Future Information Technology and Management Engineering (FITME), 2010 International Conference on*, volume 2, pages 425–428. IEEE, 2010.

[66] Ekta Walia, Chandan Singh, and Anjali Goyal. On the fast computation of orthogonal fourier–mellin moments with improved numerical stability. *Journal of Real-Time Image Processing*, 7(4):247–256, 2012.

[67] Khalid M Hosny. Fast and low-complexity method for exact computation of 3d legendre moments. *Pattern Recognition Letters*, 32(9):1305–1314, 2011.

[68] Stephane Derrode and Faouzi Ghorbel. Robust and efficient fourier–mellin transform approximations for gray-level image reconstruction and complete invariant description. *Computer vision and image understanding*, 83(1):57–78, 2001.

[69] Chandan Singh and Rahul Upneja. Accurate computation of orthogonal fourier-mellin moments. *Journal of Mathematical Imaging and Vision*, 44(3):411–431, 2012.

[70] C Lakshmi Deepika, A Kandaswamy, C Vimal, and B Satish. Palmprint authentication using modified legendre moments. *Procedia Computer Science*, 2:164–172, 2010.

[71] Arup Sarmah and Chandan Jyoti Kumar. Iris verification using legendre moments and knn classifier.

[72] Emilio Marengo, Marco Bobba, Maria Cristina Liparota, Elisa Robotti, and Pier Giorgio Righetti. Use of legendre moments for the fast comparison of two-dimensional polyacrylamide gel electrophoresis maps images. *Journal of Chromatography A*, 1096(1):86–91, 2005.

[73] S Sreehari Sastry, K Mallika, B Gowri Sankara Rao, Sie Tiong Ha, and S Lakshminarayana. Novel approach to study liquid crystal phase transitions using legendre moments. *Phase transitions*, 85(8):735–749, 2012.

[74] Thawar Arif, Zyad Shaaban, Lala Krekor, and Sami Baba. Object classification via geometrical, zernike and legendre moments. *Journal of Theoretical*

and Applied Information Technology, 7(1):31–37, 2009.

[75] Mrinal K Mandal, Tyseer Aboulnasr, and Sethuraman Panchanathan. Image indexing using moments and wavelets. *IEEE Transactions on Consumer Electronics*, 42(3):557–565, 1996.

[76] Yan Zhang, Stephen J Kiselewich, and William A Bauson. Legendre and gabor moments for vehicle recognition in forward collision warning. In *Intelligent Transportation Systems Conference, 2006. ITSC'06. IEEE*, pages 1185–1190. IEEE, 2006.

[77] Hui Zhang, Huazhong Shu, Gouenou Coatrieux, Jie Zhu, QM Jonathan Wu, Yue Zhang, Hongqing Zhu, and Limin Luo. Affine legendre moment invariants for image watermarking robust to geometric distortions. *IEEE Transactions on Image Processing*, 20(8):2189–2199, 2011.

[78] Hassan Qjidaa and L Radouane. Robust line fitting in a noisy image by the method of moments. *IEEE Transactions on Pattern Analysis and Machine Intelligence*, 21(11):1216–1223, 1999.

[79] Alban Foulonneau, Pierre Charbonnier, and Fabrice Heitz. Geometric shape priors for region-based active contours. In *Image Processing, 2003. ICIP 2003. Proceedings. 2003 International Conference on*, volume 3, pages III–413. IEEE, 2003.

[80] A Ahmadian, E Faramarzi, et al. Image indexing and retrieval using gabor wavelet and legendre moments. In *Engineering in Medicine and Biology Society, 2003. Proceedings of the 25th Annual International Conference of the IEEE*, volume 1, pages 560–563. IEEE, 2003.

[81] Rongfang Luo and Tusheng Lin. Finger crease pattern recognition using legendre moments and principal component analysis. *Chinese Optics Letters*, 5(3):160–163, 2007.

[82] Ban-Hoe Kwan, Kok-Meng Ong, and Raveendran Paramesran. Noise removal of ecg signals using legendre moments. In *Engineering in Medicine and Biology Society, 2005. IEEE-EMBS 2005. 27th Annual International Conference of the*, pages 5627–5630. IEEE, 2006.

[83] Khalid M Hosny, George A Papakostas, and Dimitris E Koulouriotis. Accurate reconstruction of noisy medical images using orthogonal moments. In *Digital Signal Processing (DSP), 2013 18th International Conference on*, pages 1–6. IEEE, 2013.

[84] Chee-Way Chong, Paramesran Raveendran, and Ramakrishnan Mukundan. Translation and scale invariants of legendre moments. *Pattern recognition*, 37(1):119–129, 2004.

[85] George A Papakostas, Evangelos G Karakasis, and Dimitris E Koulouriotis. Accurate and speedy computation of image legendre moments for computer

vision applications. *Image and Vision Computing*, 28(3):414–423, 2010.

[86] Khalid M Hosny. Refined translation and scale legendre moment invariants. *Pattern Recognition Letters*, 31(7):533–538, 2010.

[87] Khalid M Hosny. Exact legendre moment computation for gray level images. *Pattern Recognition*, 40(12):3597–3605, 2007.

[88] Huazhong Shu, Limin Luo, Xudong Bao, Wenxue Yu, and Guoniu Han. An efficient method for computation of legendre moments. *Graphical Models*, 62(4):237–262, 2000.

[89] GY Yang, HZ Shu, Christine Toumoulin, Guo-Niu Han, and Limin M Luo. Efficient legendre moment computation for grey level images. *Pattern Recognition*, 39(1):74–80, 2006.

[90] JD Zhou, HZ Shu, LM Luo, and WX Yu. Two new algorithms for efficient computation of legendre moments. *Pattern Recognition*, 35(5):1143–1152, 2002.

[91] Li Ma, Tieniu Tan, Yunhong Wang, and Dexin Zhang. Local intensity variation analysis for iris recognition. *Pattern recognition*, 37(6):1287–1298, 2004.

[92] Pravin S Patil. Iris recognition based on gaussian-hermite moments. *International Journal on Computer Science and Engineering*, 4(11):1794, 2012.

[93] Bo Yang and Mo Dai. Image reconstruction from continuous gaussian–hermite moments implemented by discrete algorithm. *Pattern Recognition*, 45(4):1602–1616, 2012.

[94] Lin Wang and Mo Dai. Application of a new type of singular points in fingerprint classification. *Pattern recognition letters*, 28(13):1640–1650, 2007.

[95] Lin Wang and Mo Dai. Extraction of singular points in fingerprints by the distribution of gaussian-hermite moment. In *Distributed Frameworks for Multimedia Applications, 2005. DFMA'05. First International Conference on*, pages 206–209. IEEE, 2005.

[96] WANG Lin and DAI Mo. Localization of singular points in fingerprint images based on the gaussian-hermite moments [j]. *Journal of Software*, 17(2):242–249, 2006.

[97] Naouar Belghini, Arsalane Zarghili, and Jamal Kharroubi. 3d face recognition using gaussian hermite moments. *Spec. Issue Int. J. Comput. Appl. Softw. Eng. Databases Expert Syst*, 1:1–4, 2012.

[98] SM Mahbubur Rahman, Shahana Parvin Lata, and Tamanna Howlader. Bayesian face recognition using 2d gaussian-hermite moments. *EURASIP Journal on Image and Video Processing*, 2015(1):35, 2015.

[99] Xiaojuan Ma, Renlong Pan, and Lin Wang. License plate character recognition based on gaussian-hermite moments. In *Education Technology and*

Computer Science (ETCS), 2010 Second International Workshop on, volume 3, pages 11–14. IEEE, 2010.

[100] You ZHOU, Yan-ying LIU, Chun-min WANG, Jing CHEN, Qiu-ping CHEN, and Ya-juan WEI. Contrast research of several human motion detection algorithm [j]. *Journal of Jilin University (Information Science Edition)*, 6:017, 2009.

[101] Youfu Wu, Mo Dai, Hongmei Liu, and Gang Zhou. Discrete gaussian-hermite moments and its applications. In *Wireless Communications, Networking and Mobile Computing, 2008. WiCOM'08. 4th International Conference on*, pages 1–4. IEEE, 2008.

[102] Khalid M Hosny. Fast computation of accurate gaussian–hermite moments for image processing applications. *Digital Signal Processing*, 22(3):476–485, 2012.

[103] Hai-tao Hu and Lei Qiao. Radical harmonic fourier moments. In *Intelligent Computation Technology and Automation (ICICTA), 2011 International Conference on*, volume 1, pages 468–471. IEEE, 2011.

[104] Lunshao Chai, Honggang Zhang, Zhen Qin, Jie Yu, and Yonggang Qi. Multi-feature content-based product image retrieval based on region of main object. In *Information, Communications and Signal Processing (ICICS) 2011 8th International Conference on*, pages 1–5. IEEE, 2011.

[105] Haitao Hu and Lingqian Kong. Image recognition based on radial harmonic fourier moments and svm. In *Internet Computing for Science and Engineering (ICICSE), 2012 Sixth International Conference on*, pages 138–142. IEEE, 2012.

[106] Chandan Singh and Sukhjeet K Ranade. A high capacity image adaptive watermarking scheme with radial harmonic fourier moments. *Digital signal processing*, 23(5):1470–1482, 2013.

[107] Wang Kejia, Zhang Honggang, Ping Ziliang, et al. Chinese chess character recognition with radial harmonic fourier moments. In *Document Analysis and Recognition (ICDAR), 2011 International Conference on*, pages 1369–1373. IEEE, 2011.

[108] C Singh and R Upneja. A computational model for enhanced accuracy of radial harmonic fourier moments. In *World Congress of Engineering, London, UK*, pages 1189–1194, 2012.

[109] Ming-Kuei Hu. Visual pattern recognition by moment invariants. *IRE transactions on information theory*, 8(2):179–187, 1962.

[110] Xiao-Chen Yuan, Chi-Man Pun, and C-L Philip Chen. Geometric invariant watermarking by local zernike moments of binary image patches. *Signal Processing*, 93(7):2087–2095, 2013.

[111] Milton Abramowitz and Irene A Stegun. *Handbook of mathematical functions: with formulas, graphs, and mathematical tables*, volume 55. Courier Corporation, 1964.

[112] Alireza Khotanzad and Yaw Hua Hong. Invariant image recognition by zernike moments. *IEEE Transactions on pattern analysis and machine intelligence*, 12(5):489–497, 1990.

[113] R Mukundan and KR Ramakrishnan. Fast computation of legendre and zernike moments. *Pattern recognition*, 28(9):1433–1442, 1995.

[114] Milton Abramowitz, Irene A Stegun, et al. Handbook of mathematical functions. *Applied mathematics series*, 55(62):39, 1966.

[115] Simon Liao, Amy Chiang, Qin Lu, and Miroslaw Pawlak. Chinese character recognition via gegenbauer moments. In *Pattern Recognition, 2002. Proceedings. 16th International Conference on*, volume 3, pages 485–488. IEEE, 2002.

[116] A Chiang, S Liao, Q Lu, and M Pawlak. Gegenbauer moment-based applications for chinese character recognition. In *Electrical and Computer Engineering, 2002. IEEE CCECE 2002. Canadian Conference on*, volume 2, pages 908–911. IEEE, 2002.

[117] Gábor Szego. Orthogonal polynomials, 23. In *American Mathematical Society Colloquium Publi*, volume 79, 1939.

[118] Christopher Hirata and Uroš Seljak. Shear calibration biases in weak-lensing surveys. *Monthly Notices of the Royal Astronomical Society*, 343(2):459–480, 2003.

[119] Miklós K Dede, András Demény, and Judit Kuti Darai. Evaluation of neutron pulse measurements with granada-sibona plexiglass kernel. *Nuclear Instruments and Methods in Physics Research Section A: Accelerators, Spectrometers, Detectors and Associated Equipment*, 372(1-2):233–238, 1996.

[120] Claudio Coriano and Çetin Şavkli. Qcd evolution equations: numerical algorithms from the laguerre expansion. *Computer physics communications*, 118(2-3):236–258, 1999.

[121] Richard Askey and James Arthur Wilson. *Some basic hypergeometric orthogonal polynomials that generalize Jacobi polynomials*, volume 319. American Mathematical Soc., 1985.

[122] DEv Amos. Algorithm 644: A portable package for bessel functions of a complex argument and nonnegative order. *ACM Transactions on Mathematical Software (TOMS)*, 12(3):265–273, 1986.

[123] George Neville Watson. *A treatise on the theory of Bessel functions*. Cambridge university press, 1995.

[124] Anandhakrishnan MG Joel Hanson, Annette Joy, and Jerin Francis. Plant

leaf disease detection using deep learning and convolutional neural network. *International Journal of Engineering Science*, 5324, 2017.

[125] M Ravindra Naik and Chandra Mohan Reddy Sivappagari. Plant leaf and disease detection by using hsv features and svm classifier. *International Journal of Engineering Science*, 3794, 2016.

[126] Abrham Debasu Mengistu, Seffi Gebeyehu Mengistu, and Dagnachew Melesew Alemayehu. Image analysis for ethiopian coffee plant diseases identification. *International Journal of Biometrics and Bioinformatics (IJBB)*, 10(1):1, 2016.

[127] Basavaraj Tigadi and Bhavana Sharma. Banana plant disease detection and grading using image processing. *International Journal of Engineering Science*, 6512, 2016.

[128] Lakhvir Kaur and Vijay Laxmi. Detection of unhealthy region of plant leaves using neural network. *Disease management*, 1(05):34–42, 2016.

[129] Srdjan Sladojevic, Marko Arsenovic, Andras Anderla, Dubravko Culibrk, and Darko Stefanovic. Deep neural networks based recognition of plant diseases by leaf image classification. *Computational Intelligence and Neuroscience*, 2016, 2016.

[130] K Jagan Mohan, M Balasubramanian, and S Palanivel. Detection and recognition of diseases from paddy plant leaf images. *International Journal of Computer Applications*, 144(12), 2016.

[131] Youssef Es-saady, Ismail El Massi, Mostafa El Yassa, Driss Mammass, and Abdeslam Benazoun. Automatic recognition of plant leaves diseases based on serial combination of two svm classifiers. In *Electrical and Information Technologies (ICEIT), 2016 International Conference on*, pages 561–566. IEEE, 2016.

[132] Sanjeev S Sannakki, Vijay S Rajpurohit, VB Nargund, and Pallavi Kulkarni. Diagnosis and classification of grape leaf diseases using neural networks. In *Computing, Communications and Networking Technologies (ICCCNT), 2013 Fourth International Conference on*, pages 1–5. IEEE, 2013.

[133] Shanwen Zhang and Zhen Wang. Cucumber disease recognition based on global-local singular value decomposition. *Neurocomputing*, 205:341–348, 2016.

[134] Xilin Liu, Guoniu Han, Jiasong Wu, Zhuhong Shao, Gouenou Coatrieux, and Huazhong Shu. Fractional krawtchouk transform with an application to image watermarking. *IEEE Transactions on Signal Processing*, 65(7):1894–1908, 2017.

[135] Shanwen Zhang, Xiaowei Wu, Zhuhong You, and Liqing Zhang. Leaf image based cucumber disease recognition using sparse representation classifica-

tion. *Computers and Electronics in Agriculture*, 134:135–141, 2017.

[136] Rillian Diello Lucas Pires, Diogo Nunes Gonçalves, Jonatan Patrick Margarido Oruê, Wesley Eiji Sanches Kanashiro, Jose F Rodrigues, Bruno Brandoli Machado, and Wesley Nunes Gonçalves. Local descriptors for soybean disease recognition. *Computers and Electronics in Agriculture*, 125:48–55, 2016.

[137] Christopher JC Burges. A tutorial on support vector machines for pattern recognition. *Data mining and knowledge discovery*, 2(2):121–167, 1998.

[138] Jason Weston and Chris Watkins. Multi-class support vector machines. Technical report, Citeseer, 1998.

[139] David Hughes, Marcel Salathé, et al. An open access repository of images on plant health to enable the development of mobile disease diagnostics. *arXiv preprint arXiv:1511.08060*, 2015.

List of Publications

1. Parminder Kaur, Husanbir Singh Pannu, *"Comparative Analysis Of Continuous And Discrete Orthogonal Moments For Face Recognition"*, International Conference on Elecronics, Communication and Aerospace Technology, IEEE, pages 449-453, 2017

2. Parminder Kaur, Husanbir Singh Pannu, *"Automatic Parameter Tuning for Random Forests and Decision Trees"*, International Conference On Recent Trends in Computer Science and Information Technology, pages 367-375, 2016

Youtube Link

https://youtu.be/921xgWffprg